6.1 INTRODUCTION (some may move to ch 1)

The ideas of plate tectonics have been implicit in all of the topics discussed in earlier chapters, because plate tectonics is a spectacular surface manifestation of Earth's past and present evolution. In many ways, plate tectonics is what makes Earth different from our neighboring planets. Thus we can think of Earth as the plate tectonic planet.

The key aspect of plate tectonics is that Earth's outer shell consists of moving plates. Hence the theory of plate tectonics grew out of the recognition that continents had drifted, as proposed in its modern form based on many lines of evidence by Alfred Wegener in 1915. This idea was an old one, rooted in the striking fit of the coasts of South America and Africa noted first in the 1600's. Wegener's classic work *The Origin of Continents and Oceans* offered a variety of evidence for continental drift beyond the fit of the coasts of South America and Africa (Fig 6.1-1). One relied on the fact that glaciers moving on the earth's surface leave characteristic scratches on rocks, showing the direction the glacier moved, and identifiable sedimentary deposits at the glaciers' edges. Although at present glaciers exist in polar regions, 300 million years ago glaciers covered regions that are not at the equator. The glaciated areas can be fit back implying that they were joined and near the south pole. Another line of evidence used fossils of species that are now found in areas far apart, to argue that these areas must have been joined in the past. For example, a 275 million year old reptile (mesosaurus) is found both in East South America and West Africa, but nowhere else. Hence Wegener argued that 300 my ago all the continents were joined in a supercontinent called "Pangaea" (all land), which later drifted apart (Fig 6.1-2). This would explain the glacial data, the fit of the continents, and the fossils.

Although this theory was accepted by some geologists working in the southern hemisphere who were familiar with these rocks, geophysicists and geologists working in the northern hemisphere were highly critical of it. Skeptics pointed out that it seemed physically impossible, because it was not recognized that the mantle could flow (Section 5.4), so such motions seemed physically impossible. Thus the geological evidence was discounted, and almost fifty years passed before many types of data showed that all parts of the earth's outer shell, not just the continents, were moving.

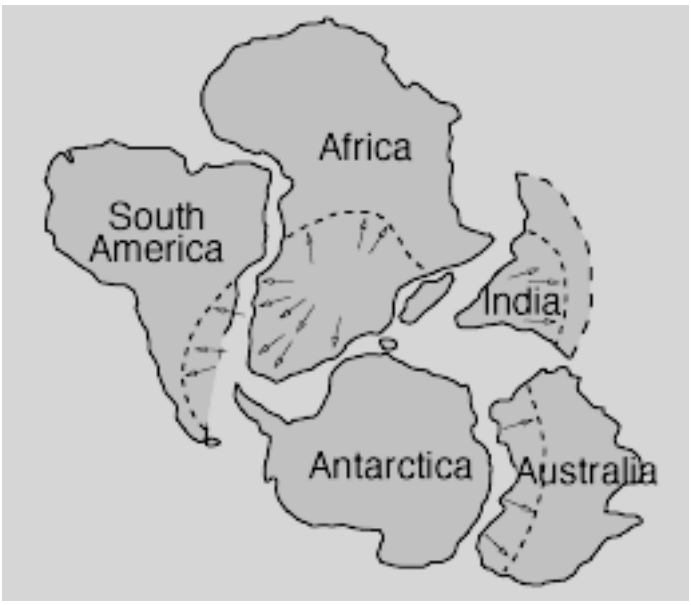

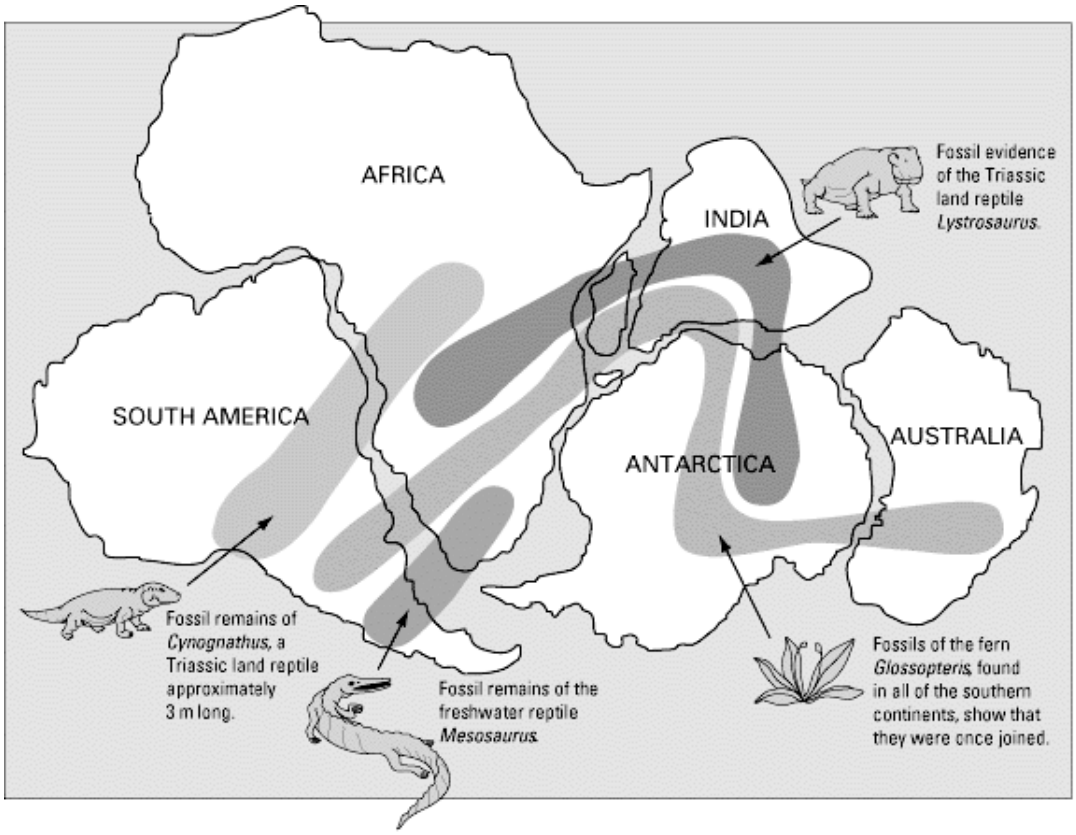

Fig 6.1-1: *Top:* Areas glaciated 300 million years fit back together implying that they were joined and near the south pole. Arrows show the direction of ice movement. *Bottom:* The areas where similar fossils are found on different continents fit together (USGS).

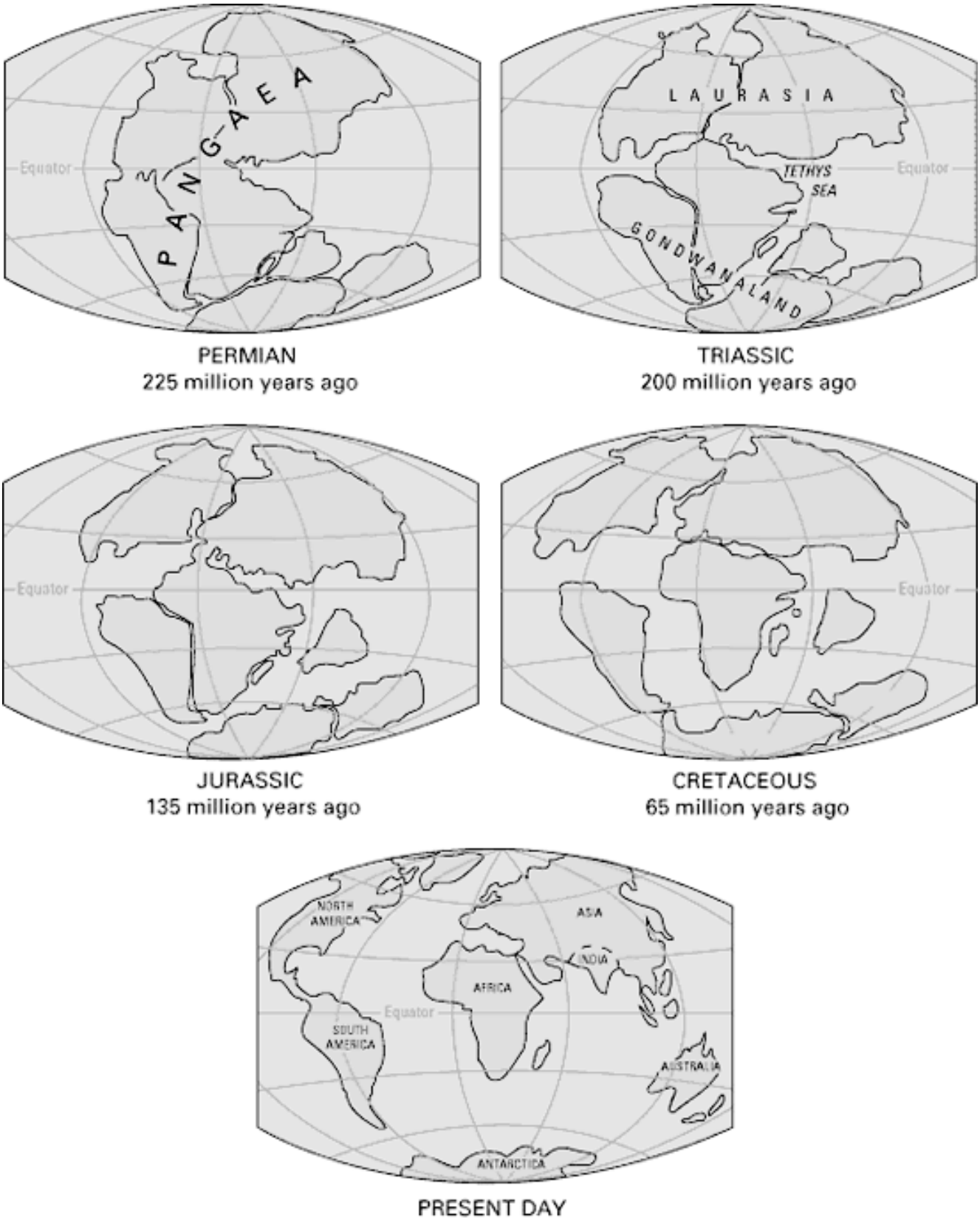

Fig. 6.1-2: Reconstruction of the supercontinent of Pangaea and the motions of the continents since its breakup (USGS).

Hence the theory of plate tectonics[1] treats the earth's outer shell as made up of about 15 major plates, and about 40 minor plates, which move relative to each other at speeds of a few centimeters per year.[2] The plates are rigid in the sense that little (ideally no) deformation occurs within them, so deformation occurs at their boundaries, giving rise to earthquakes, mountain building, volcanism, and other spectacular phenomena. These strong plates form the earth's *lithosphere,* which is about 100 km thick, and move over the weaker *asthenosphere* below. The lithosphere and asthenosphere are mechanical units defined by their strength and the way they deform. The lithosphere includes both the crust and part of the upper mantle, which are regions identified by differences in seismic velocity (chapter 3) that are thought to be chemically and mineralogically distinct.

Studies of plate tectonics are typically divided into *plate kinematics,* assessing the directions and rates of plate motions, and *plate dynamics,* understanding the forces causing plate motions. The first can be directly observed, as discussed in this chapter. The kinematics are the primary constraint on the dynamics, together with inferences from topography, seismic velocity, heat flow, gravity, and other data, which we discuss in Chapter 7.

6.1.1 Plate boundaries

Because plate tectonics is based on plate motions, plate boundaries are classified into three types depending on the relative motion between the two plates at the boundary. At *divergent boundaries* the plates move away from each other, whereas at *convergent boundaries* the plates move toward each other. At the third boundary type, *transform faults*, relative plate motion is parallel to the boundary.

These are easiest to visualize for oceanic lithosphere (Fig 6.1-3). At divergent oceanic boundaries, known as mid-ocean ridges or spreading centers, warm mantle material upwells, cools, and is added to the two plates. The material continues cooling as the lithosphere moves away from the ridges, and eventually reaches divergent boundaries, known as subduction zones or trenches. Here it

[1] Plate tectonics is a scientific theory in that it is a model of the physical world based on observations, and can be tested using new data. It describes a wide range of phenomena, although it is not a full description, much as Newtonian mechanics cannot fully describe some effects that can be described only by relativity or quantum mechanics.

[2] This is about the speed at which fingernails grow.

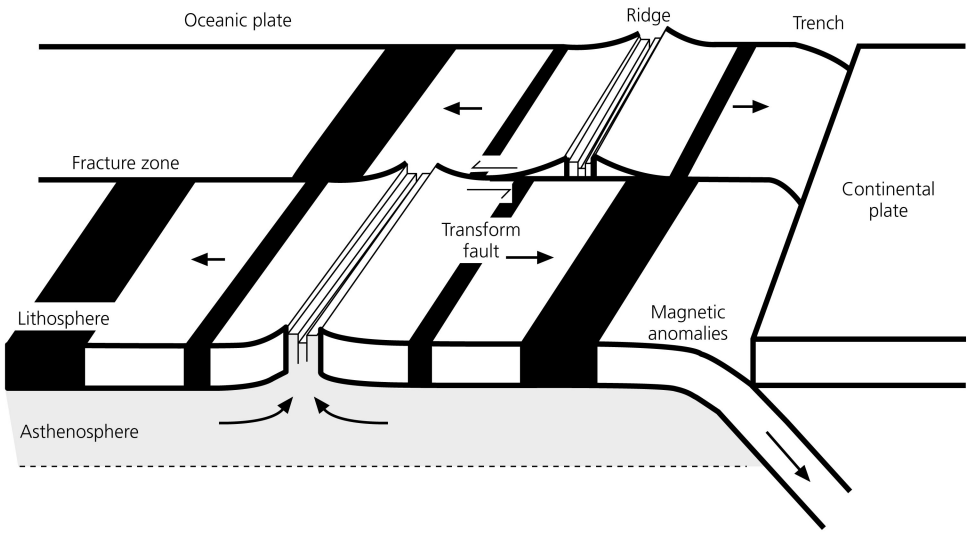

Fig. 6.1-3: Basic types of plate boundaries in oceanic lithosphere. Oceanic lithosphere is formed at ridges and subducted at trenches. At transform faults, plate motion is parallel to the boundaries.

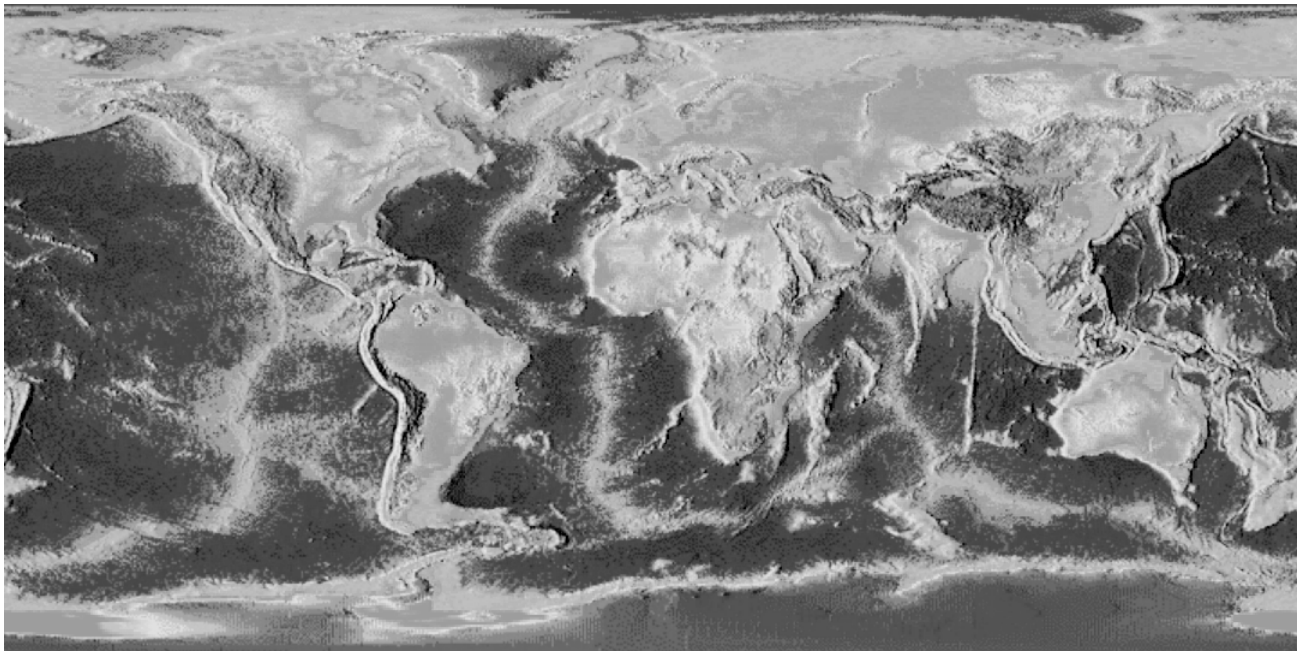

Fig 6.1-4: Most plate boundaries have a major topographic signature.

descends in downgoing slabs back into the mantle, reheating as it goes. The three boundary types also exist in the continents, but are more complicated.

Present and past plate boundaries are generally indicated by topography resulting from the boundary processes Fig 6.1-4). As a result, plate boundaries are sometimes described by their morphology. Divergent and convergent boundaries can be described either as midocean-ridges and trenches, emphasizing their morphology, or as spreading centers and subduction zones, emphasizing the plate motion there. Neither nomenclature is perfect: there are elevated features in the ocean basins that are not spreading ridges, spreading centers like the East African rift exist within continents, and continental convergent boundaries need not have a subducting slab.

Fig. 6.1-5 shows the relative motion at major plate boundaries. The relative motion at a point on the boundary determines the nature of the boundary, which often has major topographic and geological consequences. For example, the Eurasian and African plates diverge from the North American plate along the Mid-Atlantic Ridge, and convergence between the Indian and Eurasian plates produces the Himalayas and high plateau of Tibet.

An interesting consequence is that parts of the boundary between two plates can have different relative motion and thus be different boundary types. Fig. 6.1-6 shows this concept for the boundary between the Pacific and North American plates. In the south, the plates move away from the boundary, forming the Gulf of California spreading center that is rifting Baja California away from the rest of Mexico. Further north, the Pacific plate moves northwestward relative to North America along the San Andreas fault. The San Andreas fault system is essentially parallel to the relative motion, and so is largely a transform fault. In Alaska, the Pacific moves toward the boundary along the Aleutian trench and subducts beneath North America, forming the Aleutian volcanic arc. Thus this plate boundary contains ridge, transform, and trench portions depending on how the boundary is oriented relative to the plate motion.

Most plate boundaries are beautifully illustrated by the earthquakes resulting from the deformation (Fig. 6.1-7). For example, the Mid-Atlantic ridge and East Pacific rise can be followed using earthquake locations for thousands of kilometers. The trenches are even more apparent in the lower

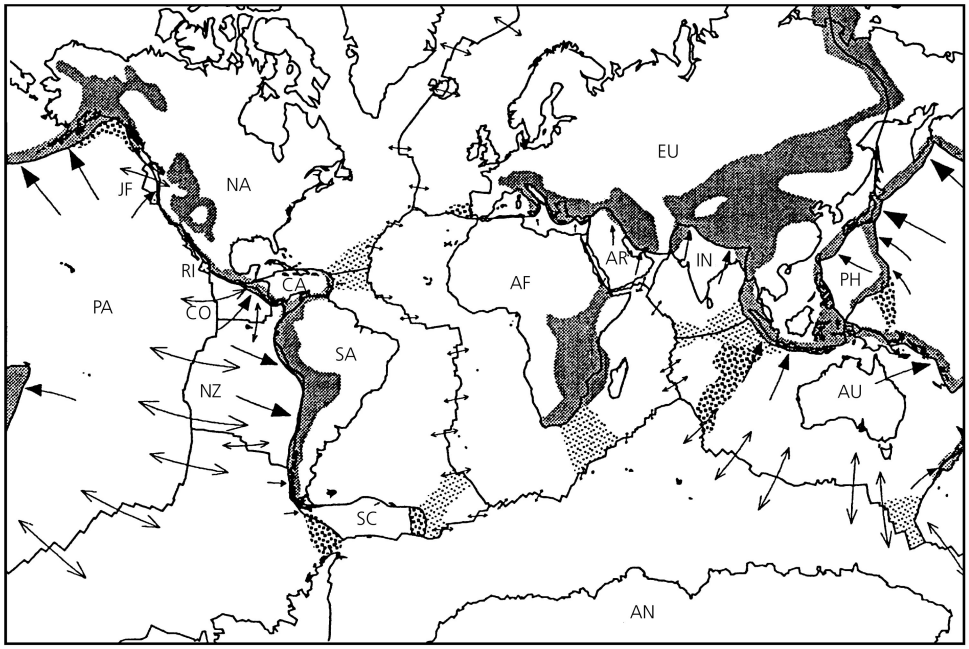

Fig. 6.1-5: Major plates and the relative motion at their boundaries. Arrow lengths are proportional to the displacement if plates maintain their present relative velocity for 25 Myr. Spreading across mid-ocean ridges is shown by diverging arrows. Convergence is shown by single arrows on the under-thrust plate. Stippled areas are diffuse plate boundary zones. (Gordon and Stein, 1992)

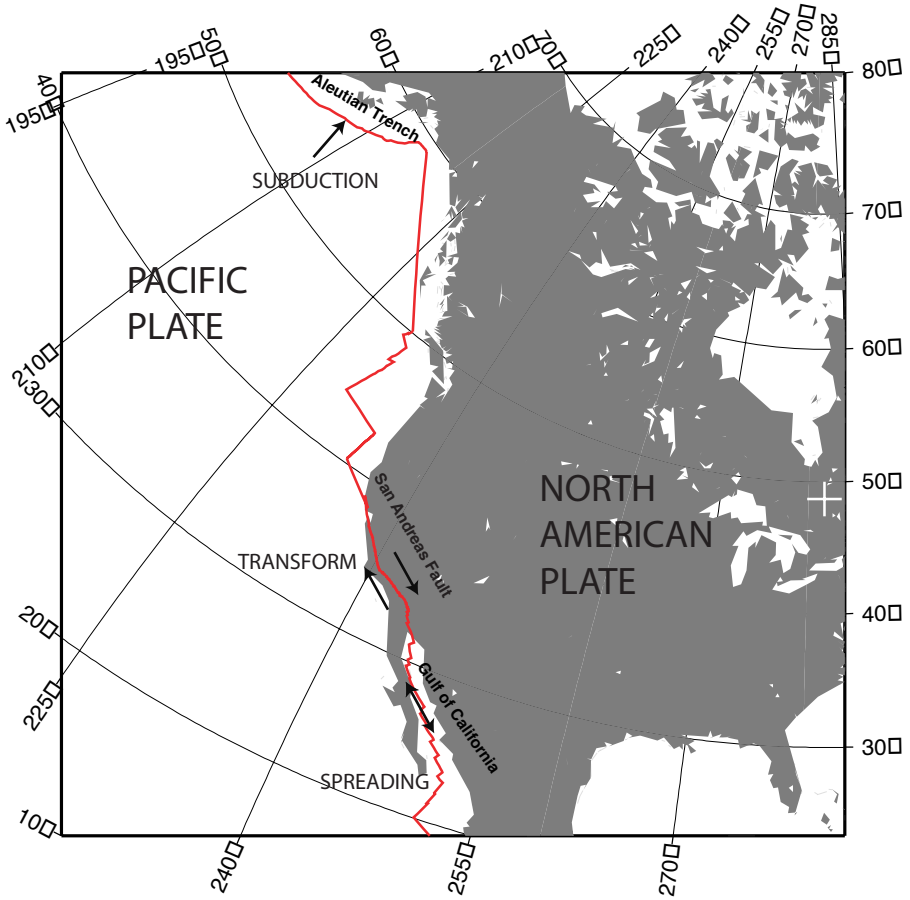

Fig. 6.1-6: Relative plate motion along the boundary between the Pacific and North American plates varies from spreading, to transform, to subduction.

panel showing earthquakes with focal depths greater than 100 kilometers, because mid-ocean ridge earthquakes are shallow and thus do not appear. In addition to delineating the boundaries, the earthquakes show the motion that occurs.

The earthquake locations also show that plate boundaries in continents are often complicated and diffuse *plate boundary zones,* rather than the simple narrow boundaries assumed in the rigid plate model that are a good approximation to what we see in the oceans. For example, seismicity shows that the collision of India with Eurasia creates a deformation zone which includes the Himalayas but extends far into China. Similarly, the northward motion of the Pacific plate with respect to North America creates a broad seismic zone, indicating that the plate boundary zone spans much of the western U.S. and Canada.

In addition, *intraplate* earthquakes occur within plate interiors, far from boundary zones. For example, Fig. 6.1-7 shows earthquakes in the central U.S., eastern Canada, northwestern Europe, and central Australia. Such earthquakes are much rarer than plate boundary zone earthquakes, but are common enough to indicate that plate interiors are not perfectly rigid. In some cases these earthquakes are associated with intraplate volcanism, as in Hawaii. Intraplate earthquakes are studied to provide data about where and how the plate tectonic model does not fully describe tectonic processes.

6.1.2 Continents and oceans

Some plates contain both continental and oceanic portions. For example, much of the North American plate consists of seafloor beneath the Atlantic Ocean. Thus the east coast of North America is a *passive continental margin,* which is not a plate boundary. Little deformation and seismicity occurs at these margins, because they are within the plate interior. There are also *active continental margins,* which are plate boundaries, such as the west coast of South America where the Nazca plate subducts beneath the South American plate, forming the high peaks of the Andes.

The continental and oceanic lithosphere have different histories due to their chemical differences. Compared to oceanic crust, continental crust is less dense (recall the differences between granitic and basaltic rocks discussed in Chapter 4), thicker (Chapter 3), and has different mechanical

properties (Chapter 7). The oceanic lithosphere is continuously subducted and reformed at ridges, and so never gets older than about 200 Myr. In contrast, the less dense continental crust does not subduct, so continental lithosphere can be billions of years old. Hence the continents preserve a complex set of geologic structures, many of which can be sites of deformation, including earthquake faulting. Thus both plate boundary and intraplate deformation zones within continents are more complex than their oceanic counterparts.

Examining plate boundaries around the world gives us examples of the different stages through which the continents and oceans have evolved. The basic process, known as the *Wilson cycle*,[3] is illustrated in Fig. 6.1-8. A continental region undergoes extension, such that the crust is stretched, faulted, and subsides, yielding a rift valley like the present East African Rift that is splitting the African plate into Nubian (west African) and Somalian (east African) plates. Because the uppermost mantle participates in the stretching, hotter mantle material upwells, causing partial melting (Chapter 4) and basaltic volcanism. Sometimes the extension stops after only a few tens of kilometers, leaving a failed or fossil rift such as the 1.2 billion year old Mid-Continent rift in the central U.S. In other cases the extension continues and the continental rift evolves into an oceanic spreading center which forms a narrow new ocean basin like the Gulf of California. With time, the ocean widens and deepens due to thermal subsidence of oceanic lithosphere (Section 5.3.3) and thick sediments accumulate on the passive continental margins, such as those on either side of the Atlantic today. Subduction often begins along one of the passive margins, and the ocean basin closes, causing magmatism and mountain building as seen along the west coast of South America today. Continental collision like that currently occurring in the Himalayas eventually occurs, and the mountain building process reaches its climax. If the continents stop moving relative to each other, the collision leaves a mountain belt within the interior of a plate. At some future time, however, a new rifting phase can begin, often near the site of the earlier rifting, and a new ocean will start to grow. Thus the Appalachian mountains record a continental collision that closed an earlier Atlantic Ocean about 270 Ma, and remain despite the opening of the present Atlantic Ocean during the past 200 Myr.

[3] Named after J. Tuzo Wilson (1908-1993), whose key role in developing plate tectonic theory included introducing the ideas of transform faults, hot spots, and that the Atlantic had closed and then reopened.

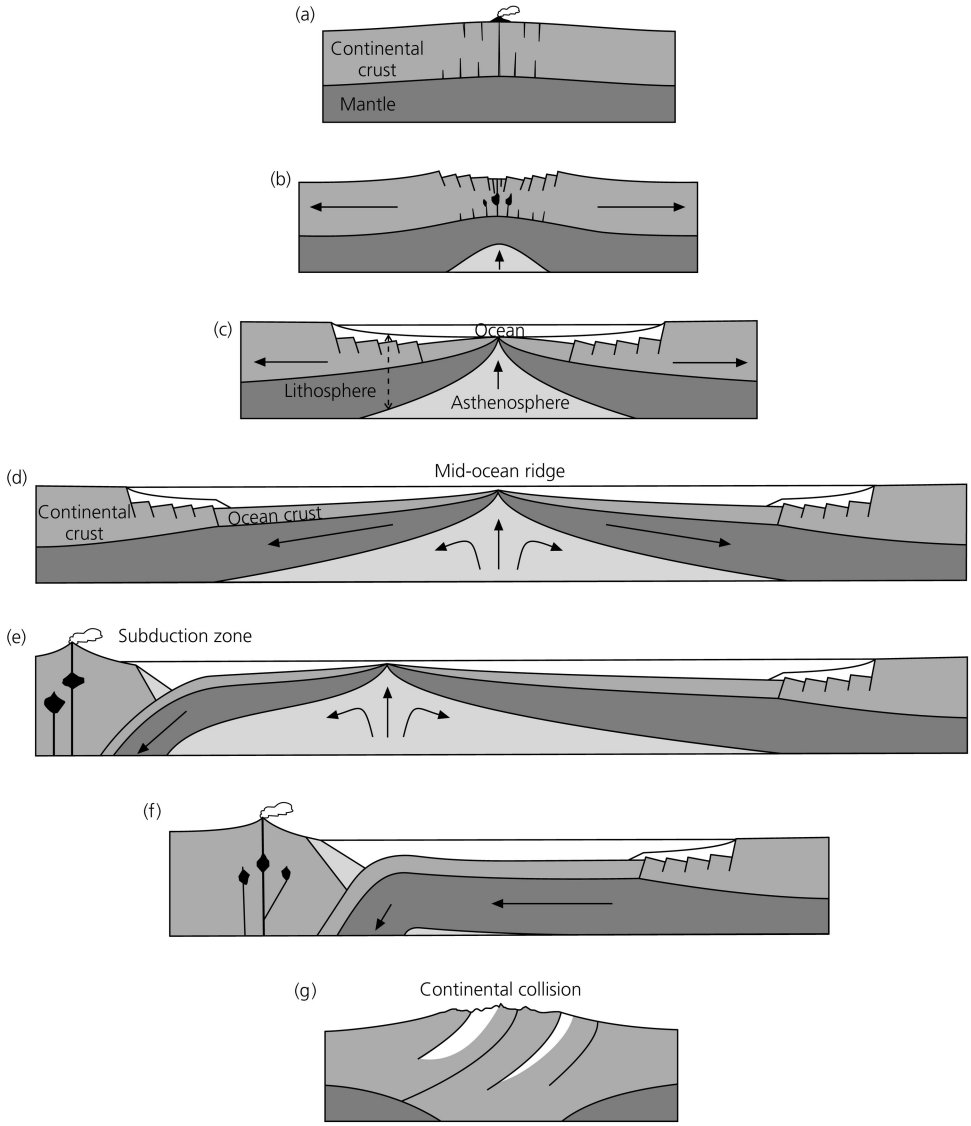

Figure 6.1-8: The Wilson cycle spans the different stages through which the continents and oceans have evolved. *a-b)* Continental stretching and rifting. *c)* Seafloor spreading begins, forming a new ocean basin. *d)* The ocean widens and is flanked by sedimented passive margins. *e)* Subduction of oceanic lithosphere begins on one of the passive margins, closing the ocean basin *(f)* and starting continental mountain building. *g)* The ocean basin is destroyed by a continental collision, which completes the mountain building process. At some later time, continental rifting begins again.

6.2 PLATE MOTIONS ON A FLAT EARTH

6.2.1 Velocity space

As we discussed in the last section, plate boundaries are classified into three types depending on the relative motion between the two plates at the boundary. Thus the rate and direction of the motion on a boundary tells us a lot about its tectonics. To formulate this idea mathematically, we begin by considering plate motions at a point on Earth's surface, or within a small region. In this case we can neglect the curvature of the planet and treat the surface as flat. Once we understand this case, we can include the effects of the spherical earth.

The relative motion between two plates at a given point at their boundary is described by a velocity vector. As we will discuss, the velocity can be found from several different types of data. Space geodetic data, derived using the Global Positioning System (GPS) or other systems, can observe both the speed (rate) and direction (azimuth) of motion. In addition, rates of spreading are found from sea-floor magnetic anomalies, which form as the hot rock at ridges cools and acquires magnetization parallel to the earth's magnetic field. Because the history of reversals of the earth's magnetic field is known, the anomalies can be dated, so their distance from the ridge where they formed shows how fast the sea floor moved away from the ridge. The directions of motion are found from the orientations of transform faults and the slip vectors of earthquakes on transforms and at subduction zones.

A velocity vector, **v**, can be specified either by its north-south and east-west components or by its rate (magnitude) and azimuth (direction) (Fig. 6.2-1). Thus

$$\mathbf{v} = (v^{NS}, v^{EW}) \tag{1}$$

has rate

$$v = |\mathbf{v}| = ((v^{NS})^2 + (v^{EW})^2)^{1/2} \tag{2}$$

and azimuth, given by the angle α measured clockwise from North

$$\alpha = \tan^{-1}(v^{EW}/v^{NS}). \tag{3}$$

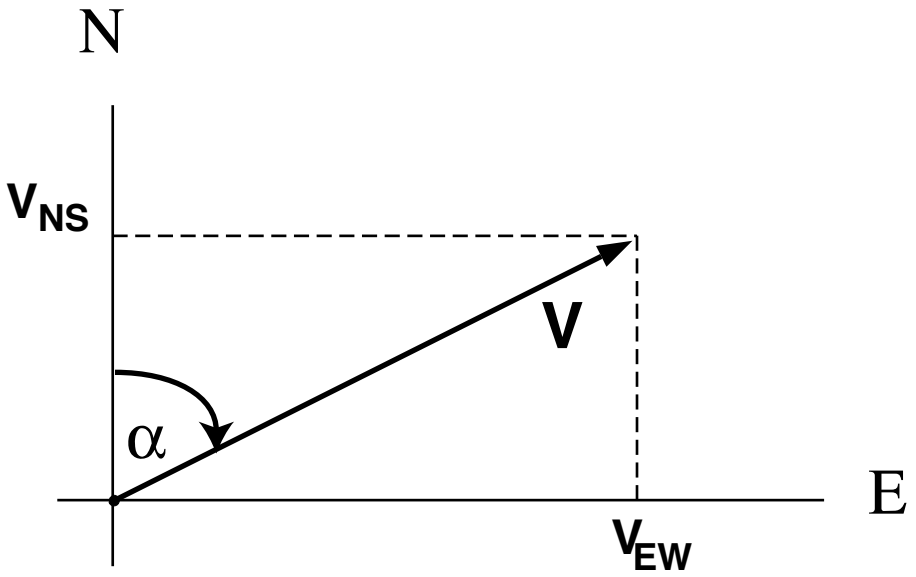

Fig. 6.2-1: A velocity vector v is speciåed either by its north-south and east-west components or by its rate (magnitude) v and azimuth (direction) α.

Conversely, the components are given by the rate and azimuth

$$v^{NS} = v\cos\alpha \quad \text{and} \quad v^{EW} = v\sin\alpha. \tag{4}$$

Two points about this notation are worth noting. The N-S and E-W components are labeled with superscripts, rather than the usual subscripts, so subscripts can be used to identify the plates involved. Also, we use the geographical convention of defining the azimuth, or angle clockwise from North. This differs from the mathematical convention of measuring the angle clockwise from the x (in this case $E-W$) direction.

Typical rates of plate motion are mm/yr or cm/yr.[1] An advantage of using mm/yr is that this is the same as kilometers per million years, so it is easy to see how the plate motion causes significant motions on the surface. For example, at a point on the San Andreas fault where the Pacific plate moves at 36 mm/yr relative to North America, rocks presently next to each other will be offset by 36 km after a million years.

We plot the relative motion between plates in a *velocity space* diagram. The diagram's axes are the north-south and east-west components of the relative motion. For example, Fig. 6.2-2a shows that plate B is moving eastward at a rate (or speed) v_{BA} relative to plate A. To plot this, we put plate A at the origin, because this plate is not moving relative to itself. The motion of plate B relative to plate A is shown by a vector $\mathbf{v}_{BA}$ whose "tail" is at the origin. Here $\mathbf{v}_{BA}$ has a direction eastward and length (magnitude) v_{BA}. To see this, imagine standing on plate A and seeing which way and how fast plate B is moving relative to you.

Because the plate motions are relative, we can also consider plate B to be fixed and plot the velocity digram (Fig. 6.2-2b) with B at the origin. The velocity vector for plate A with respect to B is the negative of that for plate B with respect to A

$$\mathbf{v}_{AB} = -\mathbf{v}_{BA}. \tag{5}$$

This has the same magnitude ($v_{AB} = v_{BA}$) but the opposite direction, because A moves westward relative to B. All the plate motions and boundary types are the same, because it is arbitrary which plate we consider fixed. Which plate we fix changes the frame of reference, but not the motions. This

[1] This is about the rate fingernails grow.

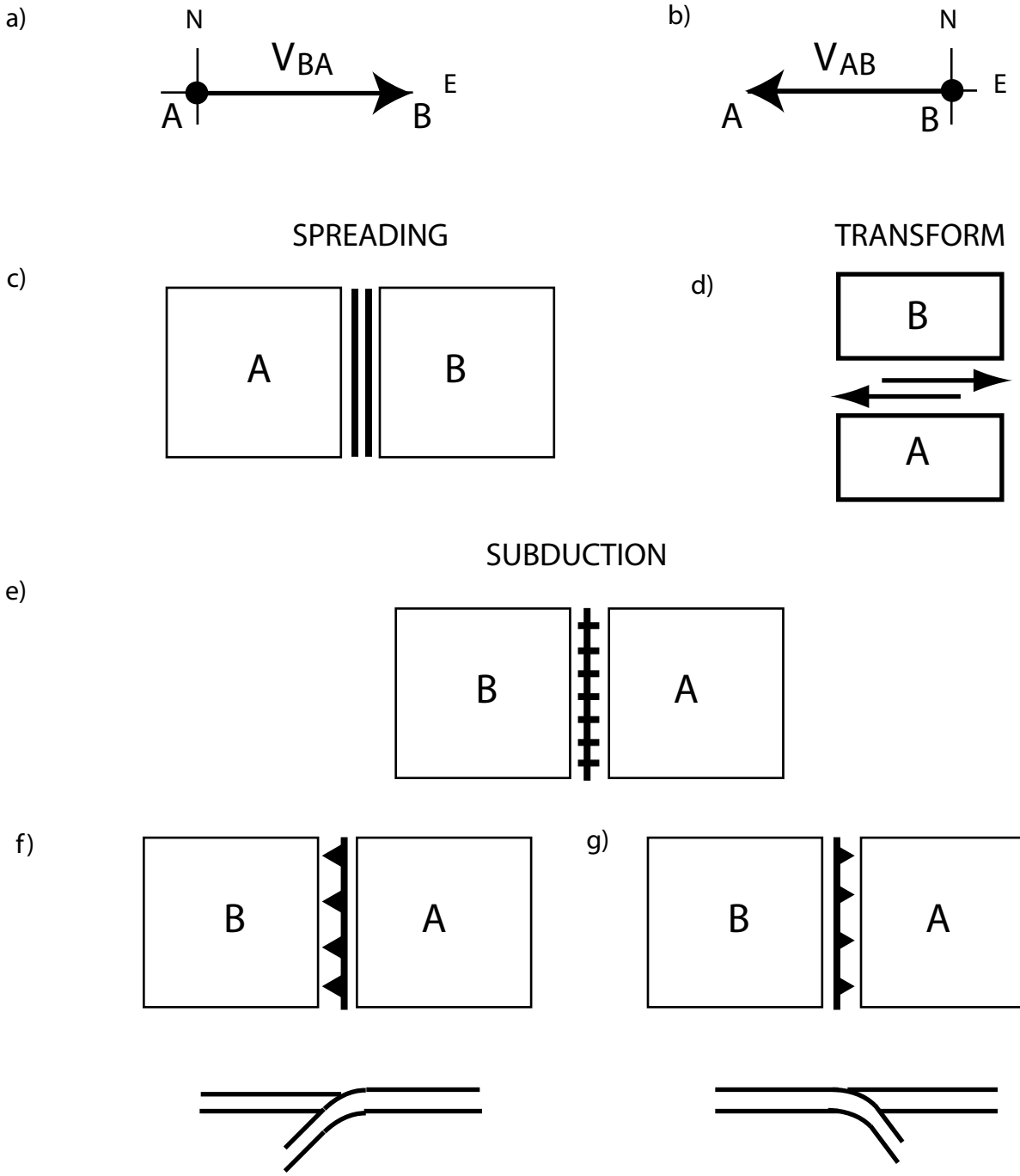

Fig. 6.2-2: Relative motion between plates. Plate B moves eastward with velocity v_{BA} relative to plate A, or plate A moves westward at v_{AB} relative to plate B. For this relative motion, the type of plate boundary depends on how the boundary is oriented compared to the relative motion vector.

makes sense because the motions are physical entities described by vectors, that are not affected by our choice of a reference frame.

What happens on a plate boundary depends on how the boundary section is oriented compared to the relative motion vector. For example, in Fig. 6.2-2c plate B is to the east and the boundary is oriented north-south. Hence along this boundary, the eastward motion of plate B moves it away from plate A. This is then a divergent boundary, a spreading center or ridge. Such boundaries are indicated by a double parallel-line symbol.

For the same relative motion, different boundary geometries can occur. A second case is illustrated in Fig. 6.2-2d, in which plate B is to the north and the boundary is oriented east-west. Because the eastward motion of plate B moves it along the boundary, the boundary is a transform fault along which material is neither added or subducted. The motion is right-lateral strike-slip, which means the motion occurs along the transform fault such that no matter which side we stand on, a point across the fault moves to the right, as indicated by the arrows.

A third possibility is that the boundary has a north-south orientation but plate A is to the east. In this case the eastward motion of plate B causes it to move toward plate A (Fig. 6.2-2e-g). Thus the boundary is a convergent boundary, indicated by the hatched-line symbol. Either plate A subducts under plate B, or the reverse - both correspond to the same relative motion. To denote the polarity of the subduction, we use a line with "teeth" on the side that is not subducting.

6.2.2 Material motion

For a given plate motion, what actually happens at the plate boundaries varies. The simplest way this motion can occur is when the plates are *rigid*, which means they do not deform. Not deforming means that points within the interior of a plate do not move relative to each other, so the plate moves as a coherent entity. In this case, all deformation and relative motion occur at the boundaries between plates. As we will see, several types of data show that in general, plates behave pretty much as though they were rigid. Hence we use the *rigid plate hypothesis* in most studies of plate motions, and include the effects of deformation as a correction when needed.

At a divergent boundary where the plates are rigid, they move apart and new material is added between them. This happens at almost all midocean ridges, where new material upwells as the plates separate. The newly formed crust and upper mantle accrete to the plates on either side and move away from the ridge. As they move away the rock cools and contracts, leaving the ridge shallower than its surroundings. This is how ocean basins grow with time, which is part of the Wilson cycle (Fig. 6.1-8).

As discussed in the next chapter, reversals of the earth's magnetic field recorded in the newly formed rocks give the age of the seafloor. Seafloor spreading is approximately *symmetric,* with equal amounts of new material added to either plate. Thus *isochrons,* lines of constant age, are approximately symmetric about the ridge axis (Fig. 6.2-3a). Dividing the distance between corresponding isochrons in opposite sides of the ridge axis by their age gives the *full spreading rate,* the average rate at which new material was added during that time. Similarly, the distance between isochrons on one side divided by their age difference gives the *half spreading rate,* the average rate at which new material was added to that plate during that period. These let us look at how the spreading rate varied over time. Comparing the distances to corresponding isochrons on opposite sides of the ridge shows whether more material was added to one plate than the other, a situation called *asymmetric spreading.* Fig. 6.2-3b illustrates a ridge spreading at the same full rate as in Fig. 6.2-3a, but with the half spreading rate on the east side faster than that on the west.

The magnetic isochrons also demonstrate the motion on transform faults that offset segments of midocean ridges. As the imaginary seafloor markers (stars) in Fig. 6.2-4 show, relative motion occurs only on the active portion of the transform between the ridge segments, where material on opposite sides of the transform is on different plates. The extensions of the transform beyond the active portion are inactive *fracture zones.* No relative motion occurs, because material on both sides of the fracture zone are on the same plate. However, there is a large scarp across fracture zones because the material on opposite sides is of different ages, and thus at deeper depths. Unfortunately, some transform faults named before this distinction became clear are known as ‘‘fracture zones" along their entire length.

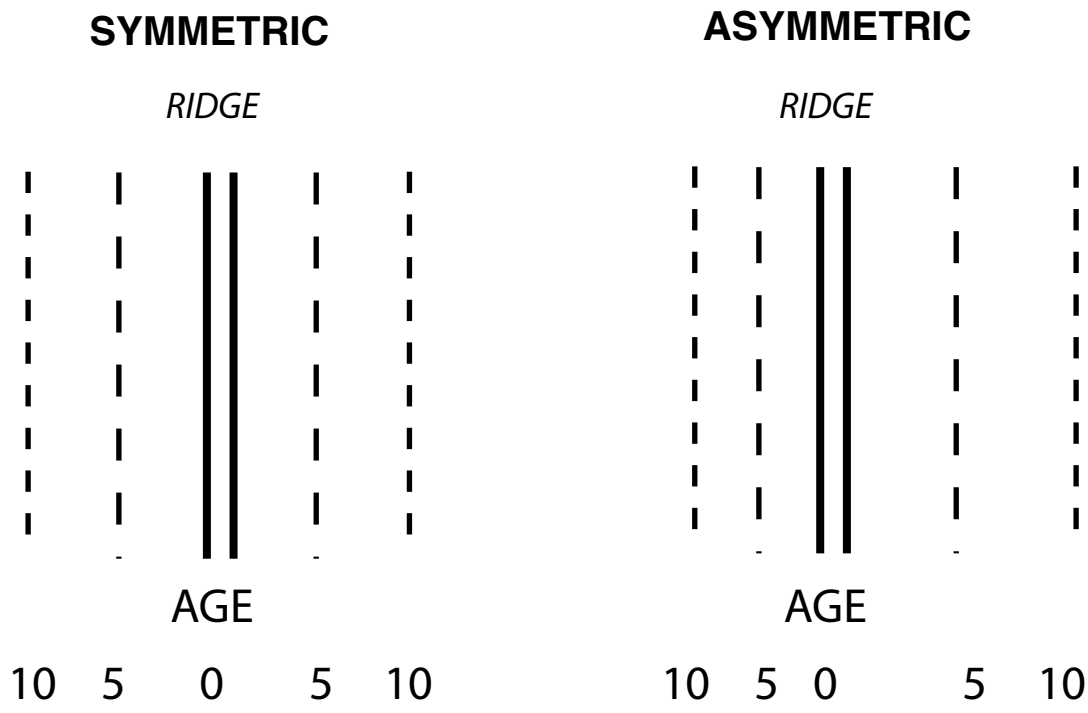

Fig. 6.2-3: Isochrons produced by symmetric (a) or asymmetric (b) seafloor spreading with the same full spreading rate.

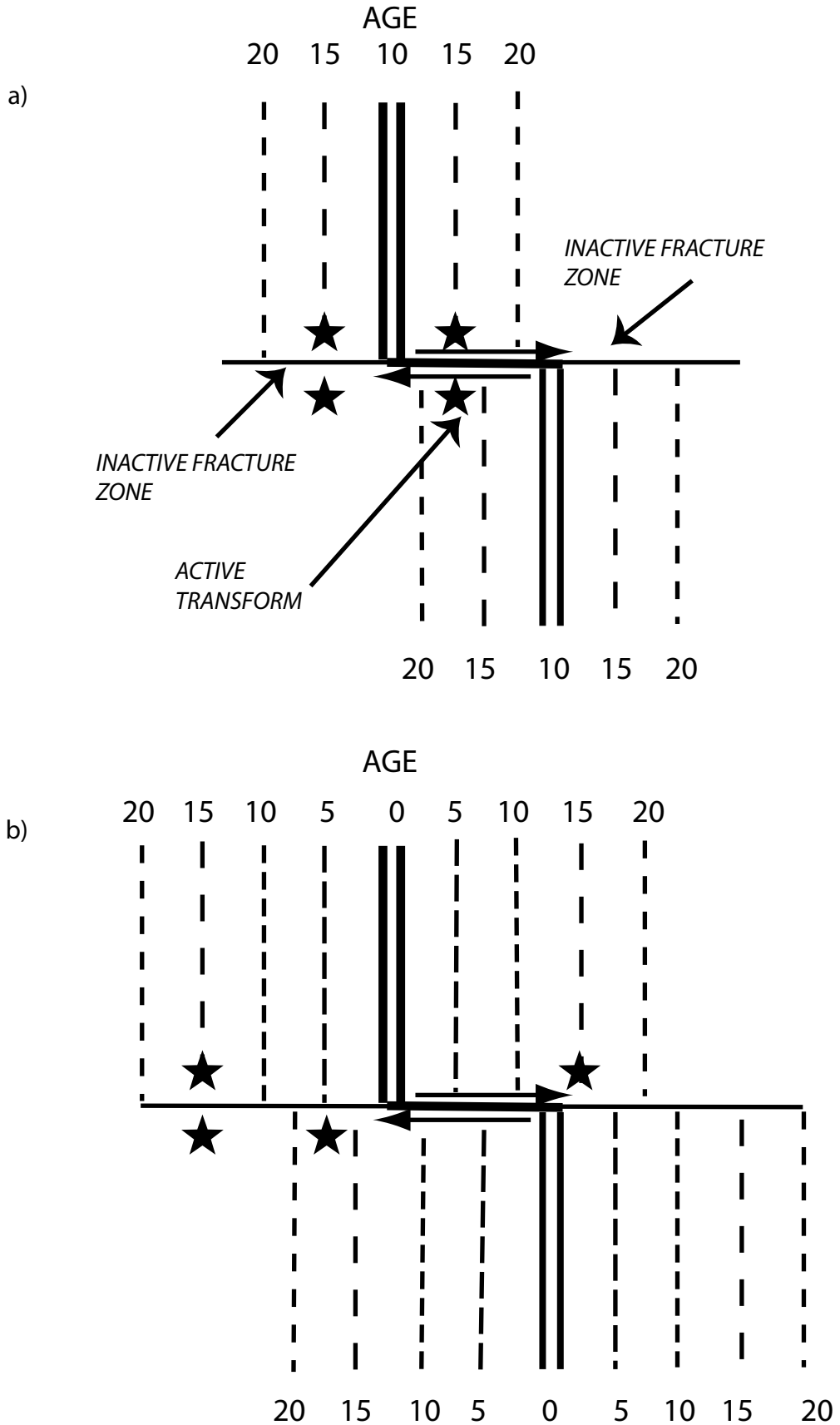

Fig. 6.2-4: Evolution of a portion of a midocean ridge-transform system, illustrated by comparison of isochrons 10 million years ago (a) and at present (b). Points on each plate, labelled with stars, illustrate relative motion across the active transform and inactive fracture zone.

A surprising feature of transform faults offsetting ridge segments results from the fact that the relative motion across the transform results from the ridges adding new material on either side. Thus the motion is not what produced the offset of the ridge crest. In the usual situation that spreading is approximately symmetric, the offset between ridge segments - which is the length of the transform - will not change with time (Fig. 6.2-5). Because transform faults offsetting ridge segments maintain essentially the same length, midocean ridges retain about the same geometry from the time they formed when continents rifted apart. Hence the Mid-Atlantic ridge reflects the shape of the continents on either side (Fig. 6.1-7).

The plate motion across a transform fault connecting spreading ridge segments results from the spreading, and so is opposite from that on strike-slip faults where the offset between features results from motion on the fault (Fig. 6.2-5). For example, the San Andreas transform fault does not offset spreading ridge segments, so the offset between features on opposite sides like stream beds grows with time.

Although ridge segments and transforms are usually about at right angles to each other, this is not always the case. Spreading is usually *orthogonal*, or in the direction of plate motion. In some cases, however, *oblique* spreading occurs (Fig 6.2-6). In either case, transforms are oriented close to the direction of plate motion, although small deviations occur. Such deviations are called *transpression*, where a small component of compression also arises, or *transtension*, where a small component of extension arises.

Motion at spreading centers can also involve a more complicated alternative, which we will discuss later, in which some of the motion occur by deforming the plates. In this geometry, which occurs when continents break apart, the continental plates on either side are stretched and thinned.

A similar situation occurs at convergent boundaries where oceanic lithosphere subducts. Because material from the subducting plate enters the trench, then over time points on the subducting plate approach the overriding plate. This is how ocean basins shrink with time, which is part of the Wilson cycle (Fig. 6.1-8).

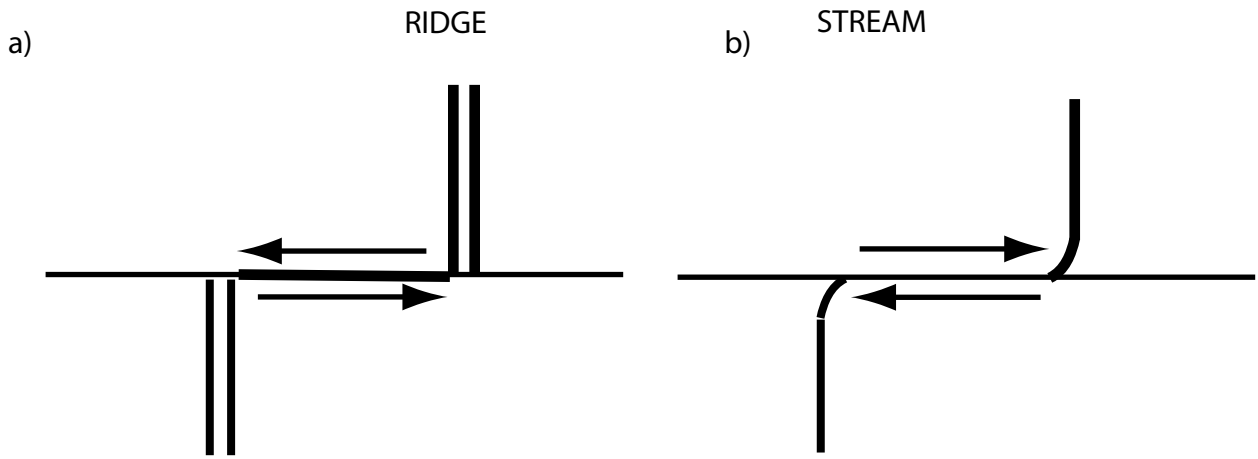

Fig. 6.2-5: The direction of motion across a transform fault connecting spreading ridge segments, whose offset does not result from motion on the fault, is opposite from that on strike-slip faults where the offset between features is produced by motion on the fault.

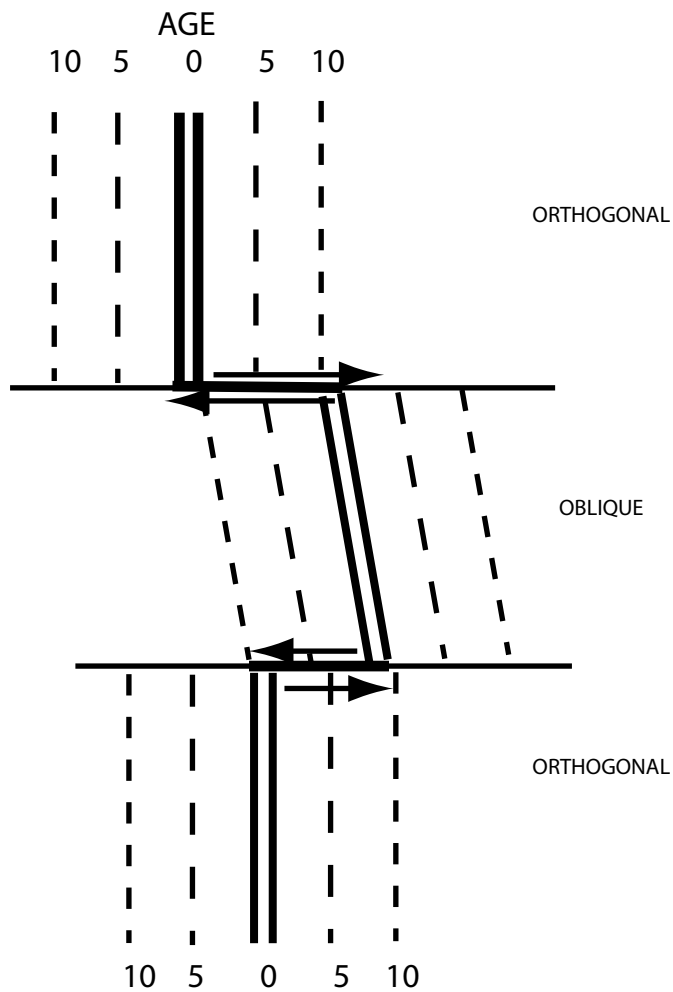

Fig. 6.2-6: The direction of plate motion is given by transforms, but seafloor spreading can be orthogonal, with ridge segments perpendicular to transforms, or oblique.

The more complicated alternative, which we will discuss later, is for some of the motion to occur by deforming the plates. This occurs when two continental plates collide, as occurs in the Himalayas.

6.2.3 Triple junctions

Velocity space analysis is often used where three plates meet at a *triple junction.* Fig. 6.2-7 shows an example, using a velocity space plot with plate B fixed. Plate A moves southeast with respect to B as shown by $\mathbf{v}_{AB}$, and plate C moves eastward with respect to B as shown by $\mathbf{v}_{CB}$.

The remaining motion, that of plate A with respect to plate C, can be found by adding and subtracting vectors. Graphically, we can see that the motion of A with respect to B is the sum of the motion of A with respect to C and the motion of C with respect to B

$$\mathbf{v}_{AB} = \mathbf{v}_{AC} + \mathbf{v}_{CB}. \tag{6}$$

Thus we can find the motion of A with respect to C from the difference

$$\mathbf{v}_{AC} = \mathbf{v}_{AB} - \mathbf{v}_{CB}. \tag{7}$$

Rewriting this gives the condition of *triple junction closure*, the requirement that the relative motions sum to zero

$$\mathbf{v}_{AC} + \mathbf{v}_{CB} - \mathbf{v}_{AB} = \mathbf{v}_{AC} + \mathbf{v}_{CB} + \mathbf{v}_{BA} = 0. \tag{8}$$

The vector addition and subtraction can be done graphically, as shown, by adding vectors "head to tail." They can also be done by adding and subtracting components, because the vector sum **w** of two vectors **u** and **v**

$$\mathbf{u} = (u^{NS}, u^{EW}) \quad \mathbf{v} = (v^{NS}, v^{EW}) \tag{10}$$

is simply

$$\mathbf{w} = (w^{NS}, w^{EW}) = (u^{NS} + v^{NS}, u^{EW} + v^{EW}) \tag{11}$$

As in the example in Fig. 6.2-2, a set of velocities can give different types of boundaries depending on the plate geometry. If plates C and A are east of B as shown in Fig. 6.2-7b, both move

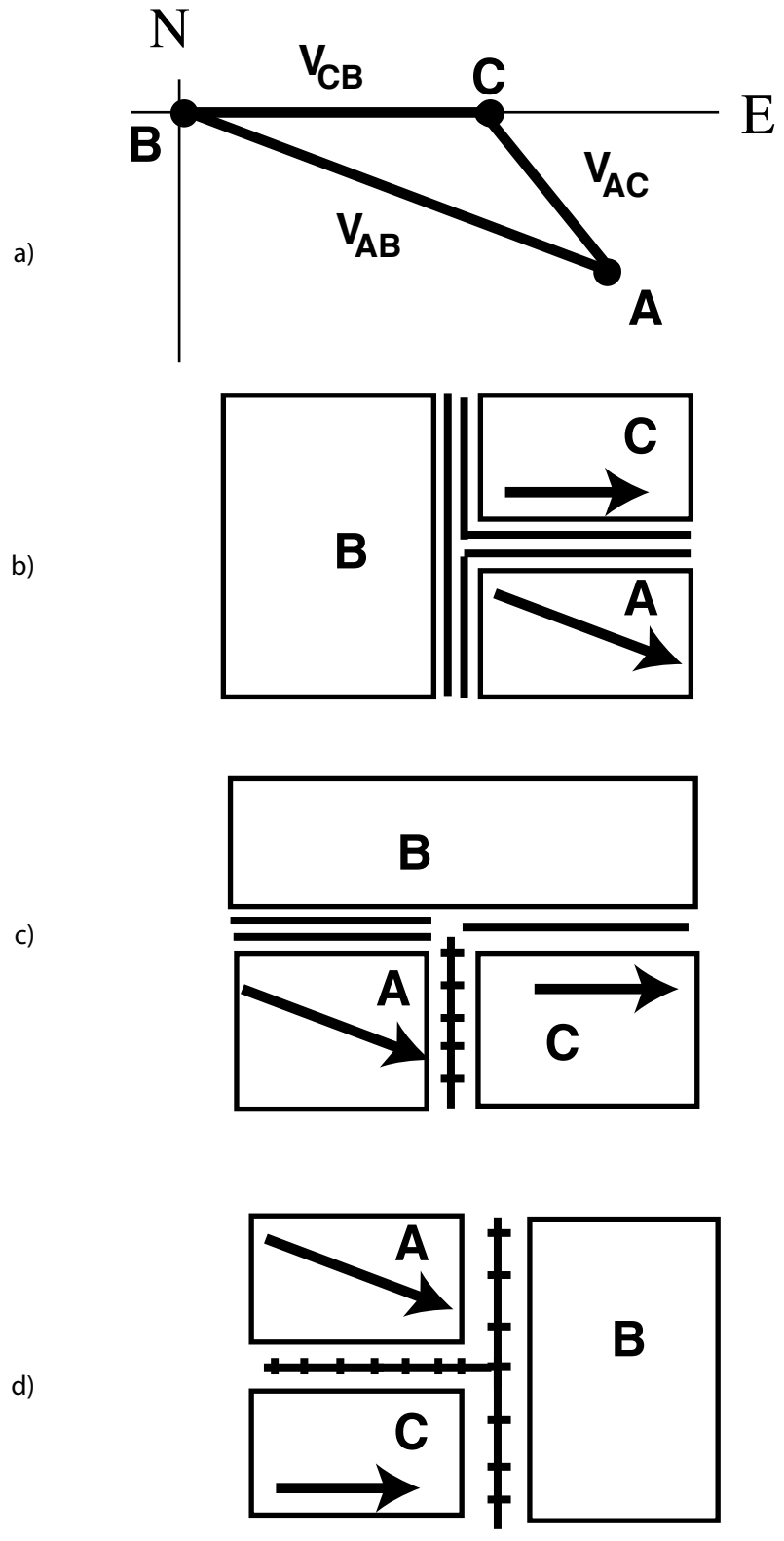

Fig. 6.2-7: a) Relative velocities with respect to plate *B* at a triple junction. b)-d) The the type of plate boundary depends on how the boundary is oriented compared to the relative motion vector, shown with respect to plate *B*.

away from B so their boundaries with B are spreading centers. Moreover, because A moves away from C, their boundary is also a spreading center. The spreading on the CB boundary is at right angles to, or orthogonal to, the boundary, whereas that on the AB and AC boundaries is oblique to the boundary.

In contrast, if plate B is north of A and C, as shown in Fig 6.2-7c, plate C's motion with respect to plate B along their boundary makes this a transform. With respect to B, plate A moves away from their boundary, making this an obliquely spreading center. However plate A moves southeast with respect to plate C, and so converges on their boundary, making this an oblique subduction zone.

Finally, if plate B is east of A and C as shown in Fig 6.2-7d, the eastward motion of plate C with respect to plate B causes orthogonal convergence along their boundary. Plate A's southeastward motion with respect to plate B makes the AB boundary obliquely convergent, and plate A's motion with respect to plate C does the same on the AC boundary.

Triple junction analysis is often used when the relative velocities on two of the three boundaries are better known than on the third, to find the motion on the third. This simple analysis of the geometry can solve puzzling tectonic questions. For example, earthquakes (Fig. 6.2-8) and topography (Fig. 6.1-4) clearly show the portion of the Mid-Atlantic ridge where spreading occurs between the African[2] plate to the east and the North and South American plates to the west. However, there is no clear evidence for the boundary between the North and South America plates. Nonetheless, analysis of spreading rates, transform fault directions, and earthquake slip vectors along the ridge, using methods discussed in the next section, indicates that these two are distinct plates with a boundary located approximately as shown by the dashed line. At the triple junction, both North and South America move east at about 23 mm/yr with respect to Africa. Subtracting these vectors gives only a small difference, about 1 mm/yr. This very slow motion on the boundary between the North and South America plates produces few earthquakes and no significant topography.

[2]Because spreading across the East African rift is slow, Africa is sometimes treated as one plate, but more detailed studies divide it into a Nubian plate west of the East African rift and a Somalian plate to the east.

a)

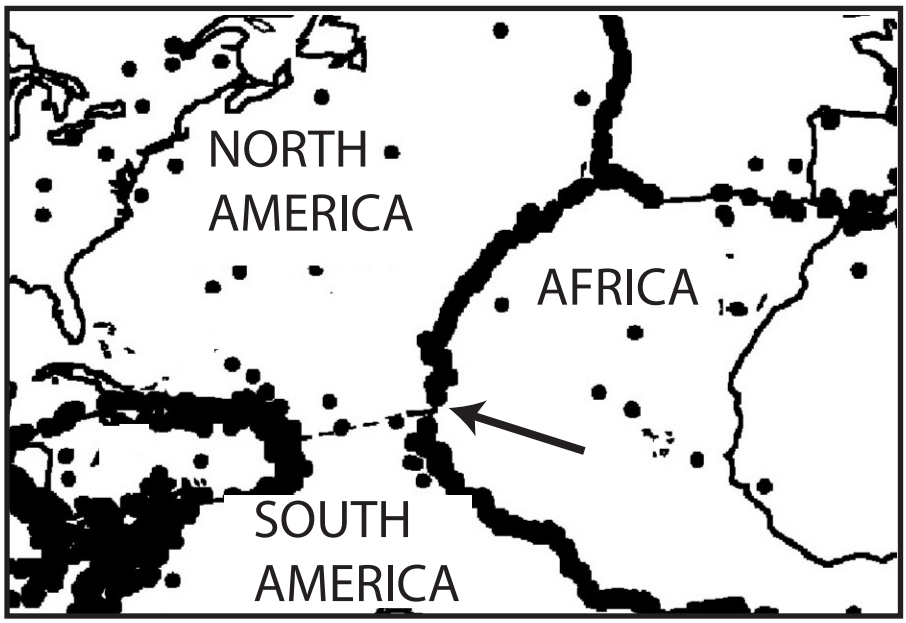

b)

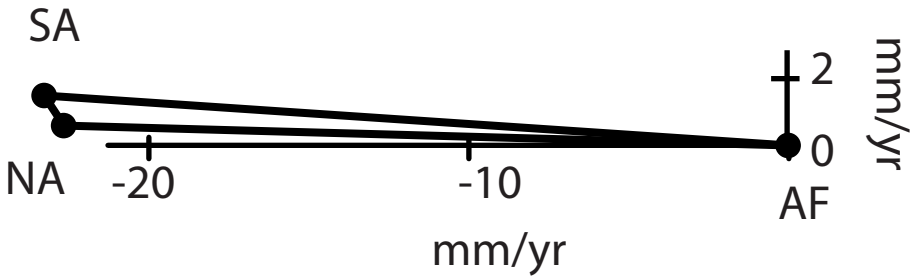

Fig. 6.2-8: a) Geometry of the triple junction between the African, North American, and South American plates. b) Relative motions at the triple junction.

Triple junction analysis resolved a puzzling question during the early studies of plate motions in western North America (Fig 6.2-9). The San Andreas fault was recognized to be a transform fault between the Pacific and North American plates. The Juan de Fuca ridge was recognized as a spreading center from seafloor magnetic anomalies. However, transform faults (labelled 3 and 4) offsetting ridge segments were not parallel to the San Andreas, whereas a transform fault to the north (#5) was. Because transform faults indicate the direction of plate motion, this difference meant that transforms #3 and #4 could not be part of the Pacific - North America boundary. Hence it seemed likely that the sea floor between the Juan de Fuca ridge and the coast was part of a separate plate, named the Juan de Fuca plate. If so, then the spreading rates and transform fault orientations on the Juan de Fuca ridge show the motion between the Pacific and Juan de Fuca plates.

How the Juan de Fuca plate moves with respect to North America is shown by the relative velocities at the triple junction (Fig. 6.2-9b). Relative to the Pacific, North America moves at 46 mm/yr to the southeast (azimuth 150°), and Juan de Fuca moves in a more easterly direction (azimuth 114°) at 54 mm/yr. The vector difference shows that Juan de Fuca moves northwestward (azimuth 56°) relative to North America at 32 mm/yr. Thus the coast is a subduction zone boundary called the Cascadia subduction zone.

This result seemed surprising, because some typical features of such subduction zones seemed missing. Subduction zones typically have deep trenches along the plate boundary, which was not seen. They also are often the sites of great earthquakes at the interface between the two plates, which were not known to have happened. On the other hand, the active Cascade volcanos, like Mt. Saint Helens, were andesitic stratovolcanos typical of those on overriding plates. Investigators soon realized that there was no obvious trench because sediments from the Columbia river filled it. Even more surprisingly, geological studies found deposits produced by a great subduction earthquake that occurred in the year 1700, which generated a major tsunami that did serious damage as far away as Japan. Finally, the fact that transform #2, the Mendocino transform, was not parallel to any of the others turned out to be because the southern part of the Juan de Fuca plate is deforming, and thus sometimes treated as a distinct Gorda plate.

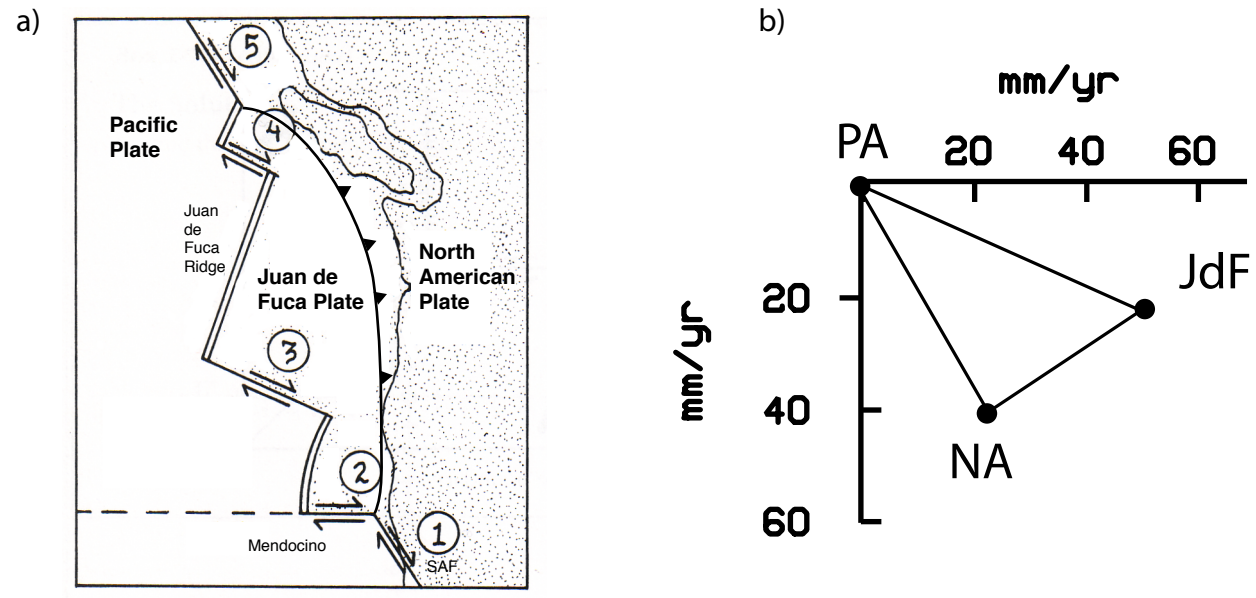

Fig. 6.2-9: a) Geometry of the Juan de Fuca, Paciåc, and North American plates. (Cox and Hart, 1986) b) Relative motions at the triple junction.

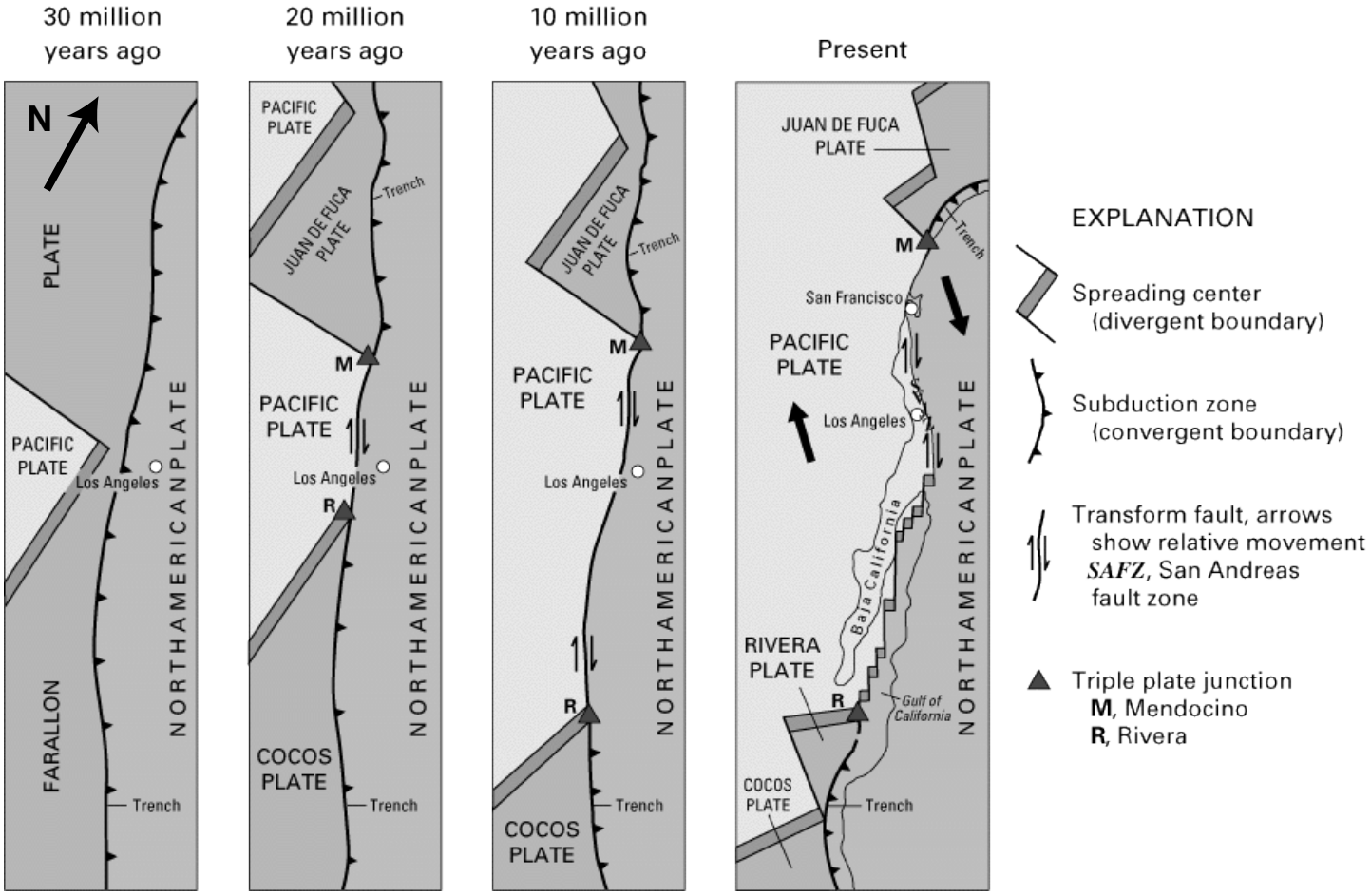

Fig. 6.2-10: Evolution of the Farallon, Pacific, and North American plates since 30 Ma. As a result of the relative motion, the Farallon plate divided into the Juan de Fuca, Cocos, and Rivera plates. The San Andreas fault formed and grew as the Mendocino and Rivera triple junctions migrated. (U.S. Geological Survey)

Triple junctions give insight into how plate boundary geometries change with time. In this case, the Juan de Fuca plate is a remnant of the much larger Farallon plate that was subducting along western North America 30 million years ago (Fig. 6.2-10). Because the Farallon plate subducted faster than new Farallon crust was produced by spreading, the spreading center approached the coast. About 25 million years ago the spreading center reached the coast, creating a new boundary between the Pacific and North American plates. Because the direction of motion between the Pacific and North American plates was parallel to this new boundary, it formed a new transform fault, the San Andreas fault. The north end of the San Andreas was the newly formed Mendocino triple junction where the northern portion of the Farallon plate, now called the Juan de Fuca plate, met the Pacific and North American plates. Similarly, its south end was the new Rivera triple junction where the southern portion of the Farallon plate, now called the Cocos plate, met the Pacific and North American plates. As subduction continued, the San Andreas grew longer and the locations of the triple junctions moved to the north and south.

As this example shows, oceanic plates change size with time. The Pacific plate grew while the Farallon plate shrank. These changes are part of the Wilson cycle (Figure 6.1-8). This example also shows how pieces of lithosphere can be transferred from one plate to another. About 5 million years ago, the southern portion of the Pacific-North America boundary moved inland and formed a new spreading center, that opened up the Gulf of California and rifted the peninsula of Baja California away from North America. Baja California, which had been part of the North American plate, then became part of the Pacific plate. We will see in section 6.4 that GPS data show that this transfer is still going on but almost completed. In addition, a piece of the Cocos plate became the small Rivera plate.

We can think of the area as a boundary zone between two large plates, the Pacific and North America, with smaller plates caught up in the boundary zone. The smaller plates are often called microplates or blocks. There isn't a precise definition as to when a small plate becomes a microplate.

Microplates are common in areas like this where a plate boundary is evolving. They often arise when a midocean ridge changes its geometry. Figure 11 shows how a segment of a ridge can propagate and take over spreading from a neighboring segment. Because finite time is required for the

new ridge segment to transfer spreading from the old one, both are active at the same time, so the area between them becomes a microplate that isn't part of either plate. The spreading rate on the new ridge is very slow at its tip and increases away from it. As a result, the microplate rotates. Ultimately the old ridge segment will die, transferring lithosphere originally on one plate to the other and leaving inactive fossil ridges on the sea floor. Both V-shaped magnetic anomalies characteristic of ridge propagation and fossil ridges are widely found in the ocean basins, showing that this is a common way that ridges reorganize.

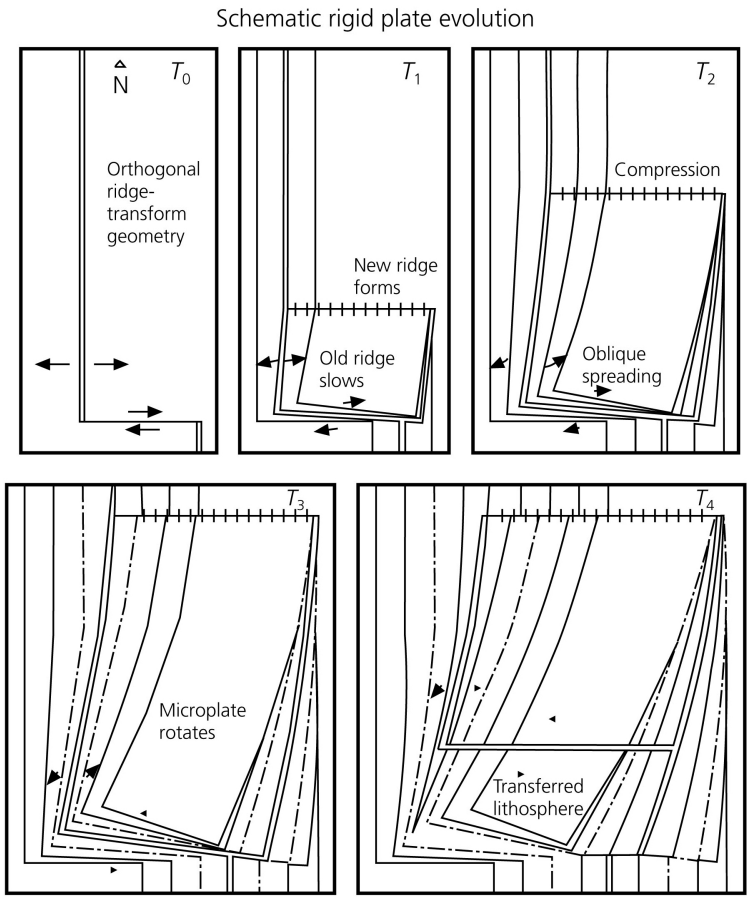

Fig. 6.2-11: Schematic model for the evolution of a rigid microplate between two major plates by rift propagation. Successive isochrons illustrate the northward propagation of the east ridge, slowing of spreading on the west ridge, the rotation of the microplate, and the transfer of lithosphere between plates (Engeln et al., 1988).

6.3 PLATE MOTIONS ON A SPHERE

6.3.1 Rotations and the cross product

In the previous section we developed the basic ideas of plate motions assuming the earth was flat. Because this approximation works only in small areas, we now extend these ideas to a spherical earth.

To do this, we use a formulation that describes an object's rotation about an axis (Fig. 6.3-1). In this, the object located by its position vector **r** rotates about an axis given by the *rotation vector* ω (also termed an angular velocity vector). The magnitude of this vector, $|\omega|$, is the *angular velocity* giving the speed of the rotation in units of angle/time.[1] The rotating object moves at a *linear velocity*

$$\mathbf{v} = \omega \times \mathbf{r} \tag{1}$$

given by the vector cross product of the rotation vector and the position vector.

By the definition of the cross product, the linear velocity vector is perpendicular to both angular velocity vector and the position vector, with direction given by the familiar right handed rule (Fig. 6.3-1). As the object moves in the direction of the linear velocity, its position vector moves with it, so the object moves in a circle about the rotation axis if the angular velocity does not change with time.

The magnitude of the linear velocity vector, or the speed of linear motion, is

$$|\mathbf{v}| = |\omega||\mathbf{r}| \sin\gamma = |\omega| l \ , \tag{2}$$

where γ is the angle between the position and rotation vectors, and $l = |\mathbf{r}| \sin\gamma$ is the distance of the point from the rotation axis. The magnitude of the position vector that describes the circular motion about the axis does not change, so the linear velocity changes direction but its magnitude stays the same. Note that for the same angular velocity, the magnitude of the linear velocity depends on the distance from the axis.[2]

---

[1] A computer's hard disk spins at about 10,000 revolutions per minute, whereas plates of earth's lithosphere rotate at about 1 degree per million years.

[2] A bicycle speedometer measures the wheel's rotation rate and finds the speed using the wheel's radius, so moving a speedometer to another bicycle without correcting for wheel size can give wildly inaccurate speeds.

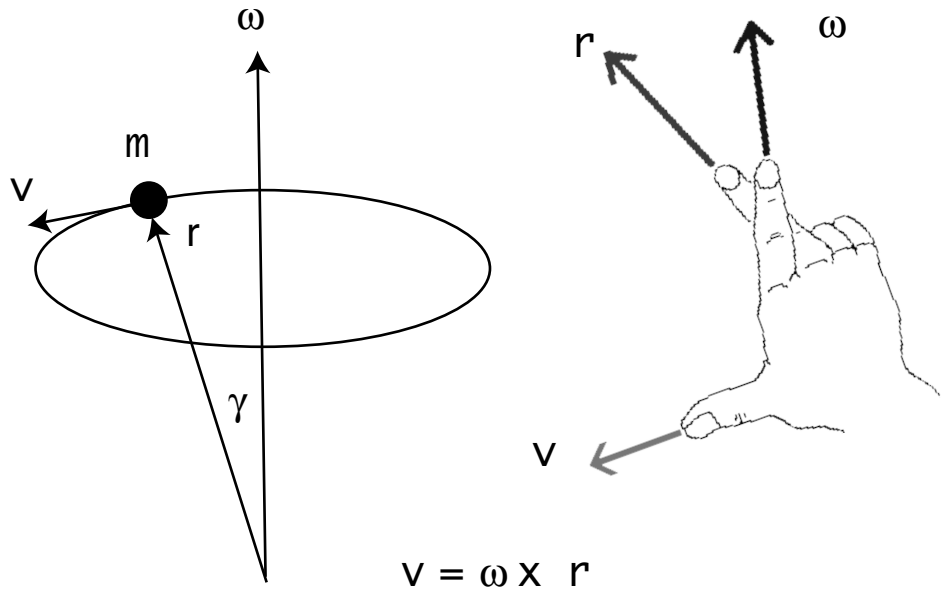

Figure 6.3-1: *Left:* The linear velocity **v** of an object rotating about an axis is the cross product of the rotation vector ω and position vector **r**. *Right:* Right handed rule: if the first and second fingers of the right hand point in the direction of the first and second vectors, the thumb points in the direction of the cross product.

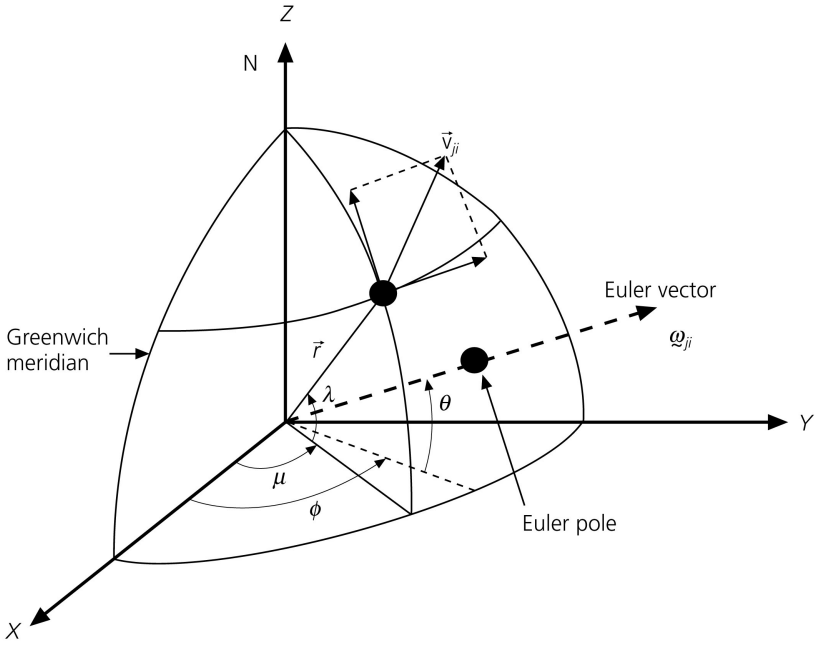

Figure 6.3-2: Geometry of plate motions. Linear velocity at point **r** is given by $\mathbf{v}_{ji} = \omega_{ji} \times \mathbf{r}$. The Euler pole is the intersection of the Euler vector with the earth's surface. Note that west longitudes and south latitudes are negative.

To evaluate the cross product, we write the vectors ω and $\mathbf{r}$ in terms of their components in a Cartesian coordinate system with x, y, z axes. The x, y, z components of the resulting vector $\mathbf{v} = \omega \times \mathbf{r}$ can be written as a row vector

$$(\mathrm{v}_x, \mathrm{v}_y, \mathrm{v}_z) = \Big((\omega_y r_z - \omega_z r_y), (\omega_z r_x - \omega_x r_z), (\omega_x r_y - \omega_y r_x) \Big) \tag{3a}$$

or a column vector

$$\begin{pmatrix} \mathrm{v}_x \\ \mathrm{v}_y \\ \mathrm{v}_z \end{pmatrix} = \begin{pmatrix} (\omega_y r_z - \omega_z r_y) \\ (\omega_z r_x - \omega_x r_z) \\ (\omega_x r_y - \omega_y r_x) \end{pmatrix}. \tag{3b}$$

A compact way is to write the cross product as the determinant

$$\mathbf{v} = \omega \times \mathbf{r} = \begin{vmatrix} \hat{\mathbf{e}}_x & \hat{\mathbf{e}}_y & \hat{\mathbf{e}}_z \\ \omega_x & \omega_y & \omega_z \\ r_x & r_y & r_z \end{vmatrix}. \tag{4}$$

The cross product of the two vectors is perpendicular to both vectors. For example, if ω and $\mathbf{r}$ are in the $x - y$ plane, their z components $\omega_z = r_z = 0$, so by equation 3 the resulting vector has only a z component. Hence the cross product is zero for parallel vectors.

6.3.2 Euler vectors for plate motions

We use the rotation geometry to describe plate motions, because a basic principle of plate tectonics is that the relative motion between any two plates can be described as a rotation about an *Euler pole*[3] (Fig. 6.3-2). Thus at any point $\mathbf{r}$ along the boundary between plate i and plate j, with latitude λ and longitude μ, the *linear velocity* of plate j with respect to plate i is

$$\mathbf{v}_{ji} = \omega_{ji} \times \mathbf{r}. \tag{5}$$

Here $\mathbf{r}$ is the position vector to the point on the boundary, and ω_{ji} is the rotation vector or *Euler vector* (also termed an angular velocity vector). Both vectors are defined from an origin at the center of

[3] This term comes from Euler's theorem, which states that the displacement of any rigid body (in this case, a plate) with one point (in this case, the center of the earth) fixed is a rotation about an axis.

center of the earth, and the *Euler pole* is the point where the Euler vector intersects Earth's surface.

The relative motion can be visualized using a geographic coordinate system whose pole is the Euler pole (Fig. 6.3-3). The direction of motion at any point on the boundary is a small circle, a parallel of latitude *about the Euler pole* (not a geographic parallel about the North Pole!). For example, in Fig. 6.3-3 (*top right*) the pole shown is for the motion of plate 2 with respect to plate 1. The convention used is that the first named plate ($j = 2$) moves counterclockwise (in a right handed sense) about the pole with respect to the second named plate ($i = 1$). The segments of the boundary where relative motion is parallel to the boundary are transform faults. Thus transforms are small circles about the pole. Other segments have relative motion away from the boundary, and are thus spreading centers. Fig. 6.3-3 (*bottom right*) shows an alternative case. The pole here is for plate 1 ($j = 1$) with respect to plate 2 ($i = 2$), so plate 1 moves toward some segments of the boundary, which are subduction zones.

The magnitude, or rate, of relative motion increases with distance from the pole because

$$|\mathbf{v}_{ji}| = |\omega_{ji}||\mathbf{r}| \sin\gamma, \tag{6}$$

where γ is the angle between the Euler pole and the site (corresponding to a colatitude about the pole). All points on a plate boundary have the same angular velocity, but the magnitude of the linear velocity varies from zero at the pole to a maximum 90° away.

Finding the motion at a point on Earth's surface involves a bit of algebra, because three different coordinate systems are involved (Fig. 6.3-2). We locate the point and the Euler pole in spherical (r, θ, ϕ) coordinates using their latitude and longitude. To find the linear velocity, we then evaluate the cross product (Eqn 5) by writing the components of the position and Euler vectors in Cartesian (x, y, z) coordinates. We then convert the linear velocity to its more useful north-south and east-west components. The reason this procedure is that (as we discussed in Chapter 2) the x, y, z axes point in the same direction at any point, but the east-west, north-south and up-down axes point in different directions at different places. Thus we cannot use the east-west, north-south and up-down axes to evaluate the cross product.

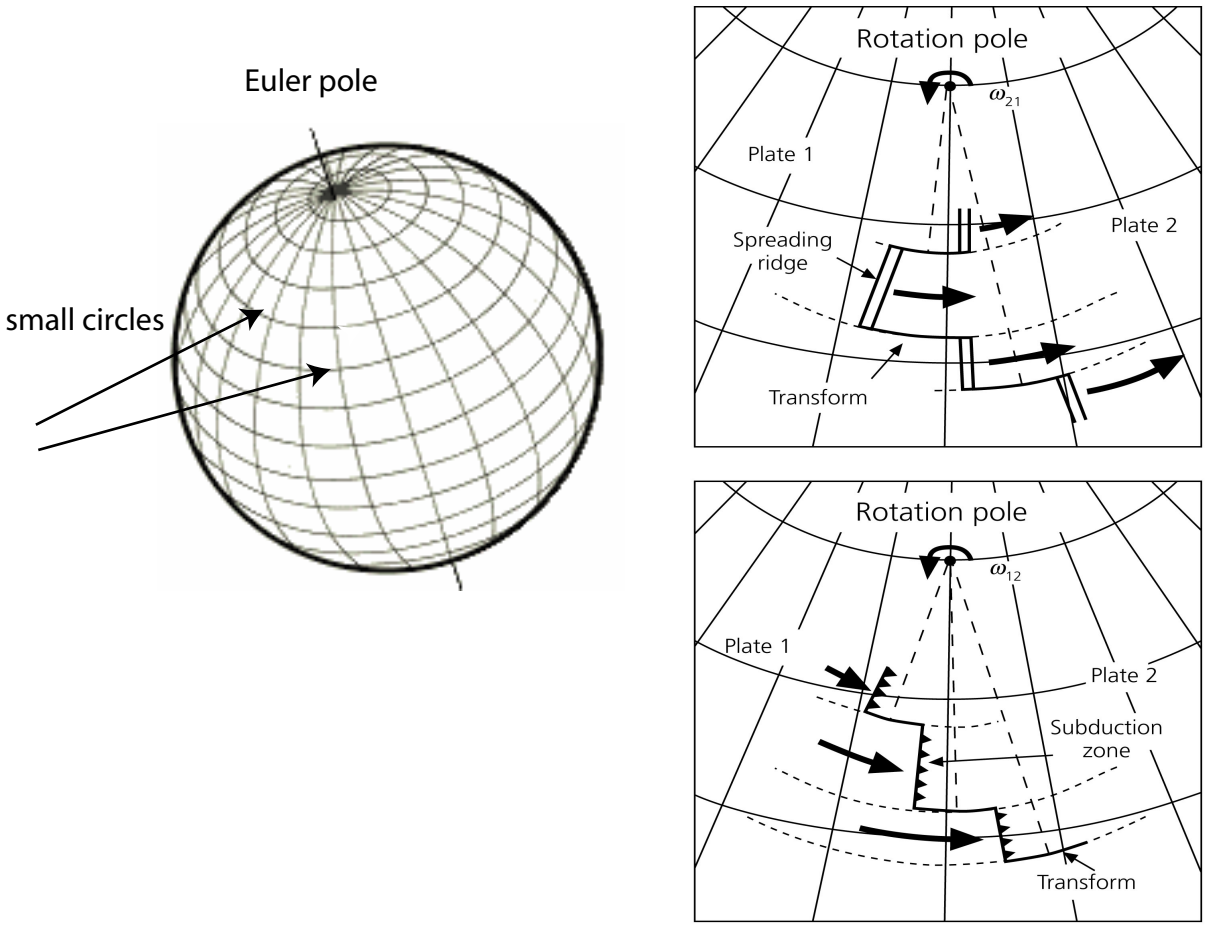

Figure 6.3-3: *Left:* Plate motions occur along small circles, parallels of latitude about the Euler pole. *Right:* Relationship of motions on plate boundaries to the Euler pole. Relative motions occur along small circles about the Euler pole (short dashed lines) at a rate that increases with distance from the pole. Note the difference the sense of rotation makes: ω_{ji} is the Euler vector corresponding to the rotation of plate j counterclockwise with respect to i.

We start by writing the position vector in Cartesian coordinates

$$\mathbf{r} = (a \cos\lambda \cos\mu,\ a \cos\lambda \sin\mu,\ a \sin\lambda), \tag{7}$$

where a is the earth's radius. Similarly, if the Euler pole is at latitude θ and longitude ϕ, the Euler vector is written (neglecting the ij subscripts for simplicity) as

$$\omega = (|\omega| \cos\theta \cos\phi,\ |\omega| \cos\theta \sin\phi,\ |\omega| \sin\theta) \tag{8}$$

where the magnitude, $|\omega|$, is the scalar angular velocity or rotation rate. To find the Cartesian components of the linear velocity **v**, we evaluate the cross product using its definition (Eqn 3), and find

$$\mathbf{v} = (\mathrm{v}_x, \mathrm{v}_y, \mathrm{v}_z), \tag{9}$$

$$\mathrm{v}_x = a|\omega| (\cos\theta \sin\phi \sin\lambda - \sin\theta \cos\lambda \sin\mu)$$

$$\mathrm{v}_y = a|\omega| (\sin\theta \cos\lambda \cos\mu - \cos\theta \cos\phi \sin\lambda)$$

$$\mathrm{v}_z = a|\omega| \cos\theta \cos\lambda \sin(\mu - \phi).$$

However, it is more useful to write these Cartesian components as north-south and east-west components. To do this, we use the north-south and east-west unit vectors derived in chapter 2

$$\hat{\mathbf{e}}^{NS} = (-\sin\lambda \cos\mu, -\sin\lambda \sin\mu, \cos\lambda) \tag{10}$$

$$\hat{\mathbf{e}}^{EW} = (-\sin\mu, \cos\mu, 0).$$

Because the component of one vector in the direction of another vector is their scalar or dot product, we find the north-south and east-west components of **v** by taking dot products of its Cartesian components (Eqn 9) with the unit vectors (Eqn 10), so

$$\mathrm{v}^{NS} = \mathbf{v} \cdot \hat{\mathbf{e}}^{NS} = a|\omega| \cos\theta \sin(\mu - \phi) \tag{11}$$

$$\mathrm{v}^{EW} = \mathbf{v} \cdot \hat{\mathbf{e}}^{EW} = a|\omega| [\cos\lambda \sin\theta - \sin\lambda \cos\theta \cos(\mu - \phi)].$$

We can then find the rate and direction of plate motion,

$$\text{rate} = |\mathbf{v}| = \sqrt{(\mathrm{v}^{NS})^2 + (\mathrm{v}^{EW})^2} \tag{12}$$

$$\text{azimuth} = 90° - \tan^{-1}[(\mathrm{v}^{NS})/(\mathrm{v}^{EW})],$$

such that azimuth is measured in the usual convention, degrees clockwise from North.

Note that there is no vertical (up-down) component of plate motion. Because the linear velocity is a cross product, it is perpendicular to the position vector r, and so in the plane of Earth's surface. However, real plates subduct into the earth and are uplifted during mountain building. Thus we use Eqns 12 to describe ideal plates moving on the surface while recognizing that vertical motions occur.

In evaluating expressions 12 for plate motions it is important to be careful with dimensions. Although rotation rates are typically reported in degrees per million years, they should be converted to radians per year. The resulting linear velocity will have the same dimensions as Earth's radius. By serendipity, converting radius in km to mm ($\times 10^6$) and Myr to years ($\times 10^{-6}$) cancel out, so only the degrees to radians ($\times \pi/180°$) conversion actually needs to be done to obtain a linear velocity in mm/yr. Plate motions are often quoted as mm/yr, because a year is a comfortable unit of time for humans and 1 mm/yr corresponds to 1 km/Myr, making it easy to visualize what seemingly-slow plate motion accomplishes over geologic time.

To see how this works, consider Fig. 6.3-4, which shows the North America-Pacific boundary zone. The map is drawn in a projection about the Euler pole, so the expected relative motion is parallel to small circles like the one shown. By analogy to Fig. 6.3-3, this geometry predicts NW-SE oriented spreading along ridge segments in the Gulf of California, which are rifting Baja California away from the rest of Mexico. Further north, the San Andreas fault system is essentially parallel to the relative motion, and so is largely a transform fault. In Alaska, the eastern Aleutian arc is perpendicular to the plate motion, so the Pacific plate subducts beneath North America. Thus this plate boundary contains ridge, transform, and trench portions depending on the geometry of the boundary.[4] In addition, the boundary zone contains the small Juan de Fuca

[4] A good way to visualize the plate motion is to photocopy Figure 4, cut along the boundary of the Pacific plate,

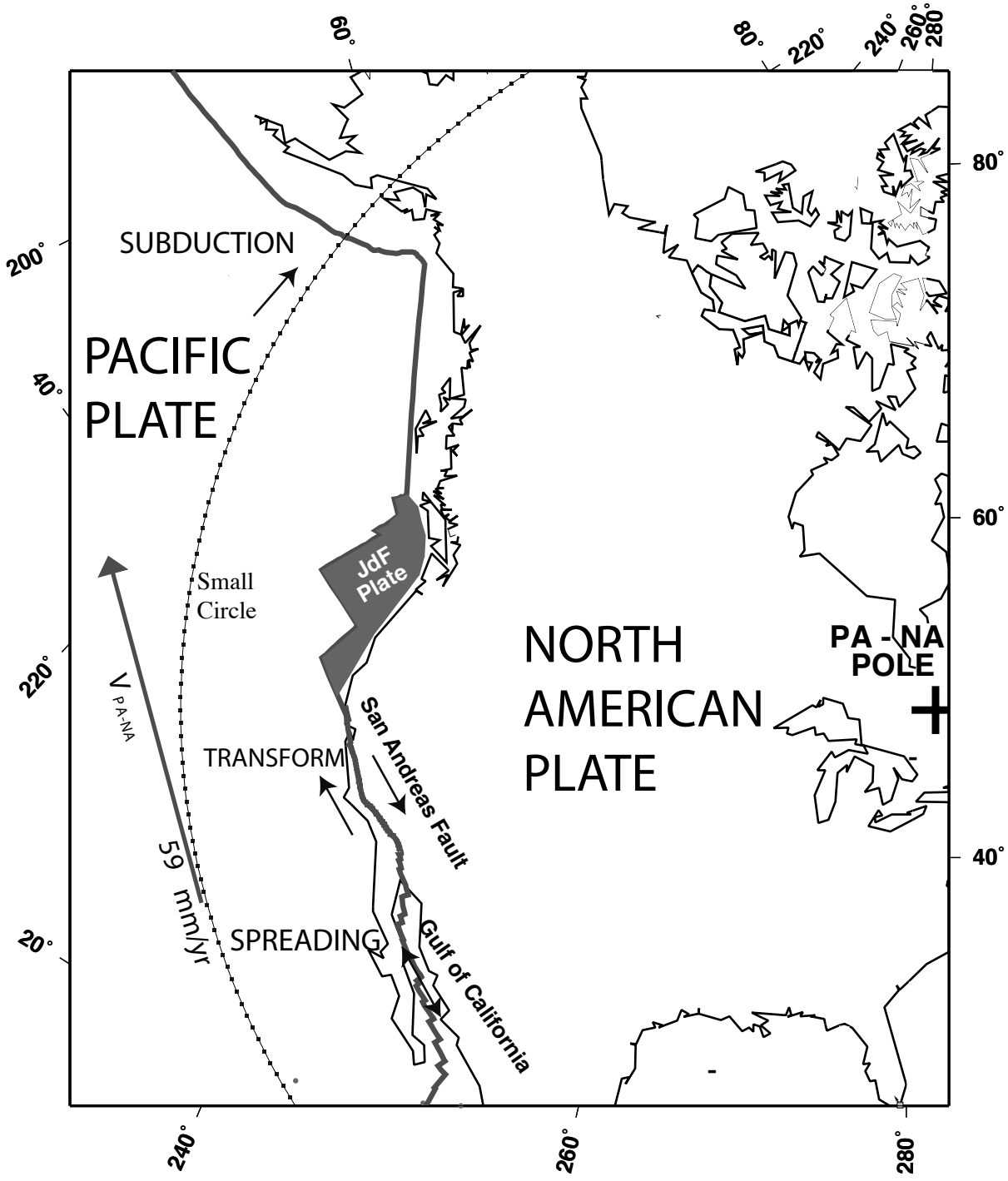

Fig. 6.3-4: Relative plate motion along the boundary between the Pacific and North American plates varies from spreading, to transform, to subduction, along small circles about the Euler pole like the one shown.

plate, which subducts beneath the Pacific Northwest.

Equation (12) lets us find how the motion varies. The predicted motion of the Pacific plate with respect to the North American plate at a point on the San Andreas fault (36°N, 121°W) has a rate of 46 mm/yr at an azimuth of N36°W. The predicted direction agrees reasonably well with the average trend of the San Andreas fault, N41°W. Thus to first order the San Andreas is a Pacific-North America transform plate boundary with right lateral motion. However, there are some deviations from pure transform behavior. As we will see, the rate on the San Andreas is less than the total plate motion because some of the motion occurs elsewhere within the broad plate boundary zone.

Similarly, at a point on the Aleutian trench near the site of the great 1964 Alaskan earthquake (62°N, 148°W), we predict Pacific motion of 53 mm/yr at N14°W with respect to North America. This motion is into the trench, which is a Pacific-North America subduction zone. As we noted in the previous section (Fig. 6.2-2), for a given convergent relative motion either plate can be subducting. However, the relative direction is important, so the plates cannot be interchanged: if N14°W were the direction of motion of North America with respect to the Pacific, the motion would be away from the boundary, which would then be a spreading center with the same rate. As for the San Andreas, the actual boundary zone shown by earthquakes and other deformation is wider and more complicated than the ideal.

6.3.3 Global plate motions

At this point you may be wondering how Euler poles are found. Until recently, this was done by combining three different types of data from different boundaries. The rates of spreading are found from sea-floor magnetic anomalies, which form as the hot rock at ridges cools and acquires magnetization parallel to the earth's magnetic field (Chapter 7). Because the history of reversals of the earth's magnetic field is known, the anomalies can be dated, so their distance from the ridge where they formed shows how fast the sea floor moved away from the ridge. The

and then photocopy the "Pacific" onto another paper. Putting the "Pacific" beneath "North America" and rotating around a thumbtack through the pole shows the ridge, transform, and trench motions both forward and backward in time.

directions of motion are found from the orientations of transform faults and directions of slip in earthquakes (Chapter 8) on transforms and at subduction zones. Euler vectors are found from the relative motion data, using geometrical conditions we have discussed.

The process is easy to visualize (Figure 6.3-5). Because slip vectors and transform faults lie on small circles about the pole, the pole must lie on a great circle at right angles to them (Figure 6.3-3). Similarly, the rate of plate motion increases with the sine of the distance from the pole (Eqn 6). These constraints make it possible to locate the poles. This was first done graphically, and is now done on a computer by finding Euler vectors for all the plates that best describe the data.

Such sets of Euler vectors are called global relative plate motion models. Because these models use spreading rates determined from magnetic anomaly data that span several million years, they describe plate motions averaged over the past few million years.[5] Another way to do this, discussed in the next section, is to use space-based observations to develop models that describe plate motion over the past few years. Comparing the two shows places where plate motions may be changing.

Table 1 gives such a model, known as NUVEL-1A,[6] which specifies the motions of plates (Figure 4) with respect to North America. The vectors follow the convention that each named plate moves counterclockwise relative to North America.

[5] The most recent magnetic reversal occurred about 780,000 years ago, so any plate model based on paleomagnetic data must average at least over that interval.

[6] NUVEL-1 (Northwestern University VELocity) was developed as a new ("nouvelle") model [*DeMets et al.*, 1990]. The multiyear development prompted the suggestion that "OLDVEL" might be a better name. Due to changes in the paleomagnetic time scale the model was revised, to NUVEL-1A [*DeMets et al.*, 1994]. This change caused a slight difference in the rates of relative motion, but not in the poles and hence directions of relative motion.

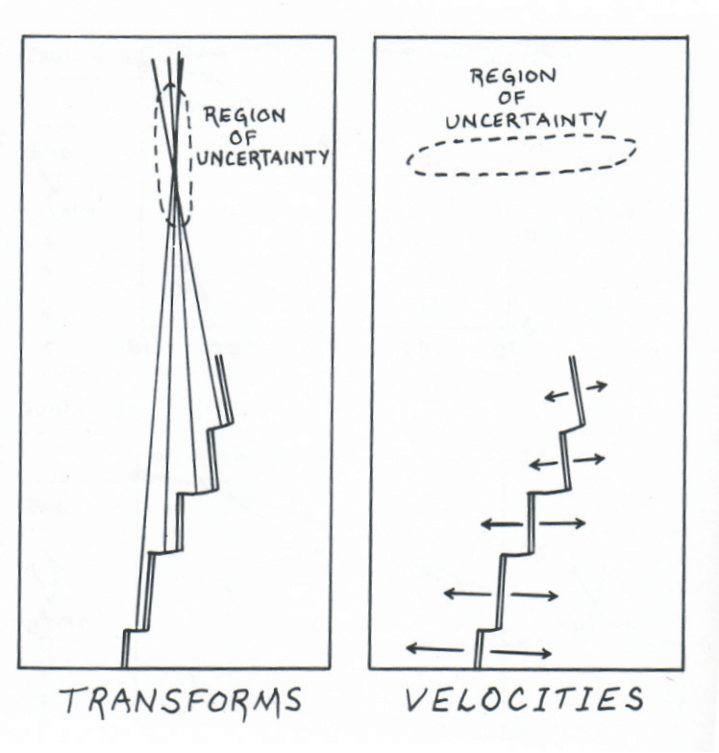

Figure 6.3-5: Graphic procedure for finding the Euler pole for relative motion between two plates. (Cox and Hart, 1986)

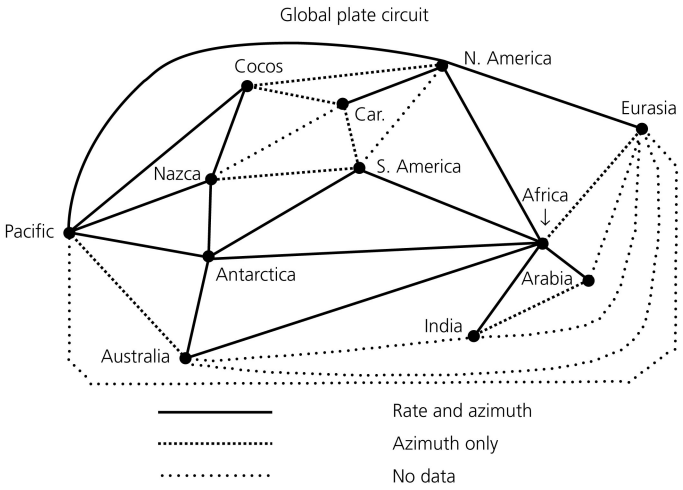

Figure 6.3-6: Global plate circuit geometry for the NUVEL-1 plate motion model. Relative motion data are used on the boundaries indicated. (Stein et al., 1986)

Table 6.3-1: Euler vectors with respect to North America (NA)

plate	pole latitude (°N)	longitude (°E)	$\|\omega\|$ (degrees/my)
PACIFIC (PA)	-48.709	101.833	0.7486
AFRICA (AF)	78.807	38.279	0.2380
ANTARCTICA (AN)	60.511	119.619	0.2540
ARABIA (AR)	44.132	25.586	0.5688
AUSTRALIA (AU)	29.112	49.006	0.7579
CARIBBEAN (CA)	74.346	153.892	0.1031
COCOS (CO)	27.883	-120.679	1.3572
EURASIA (EU)	62.408	135.831	0.2137
INDIA (IN)	43.281	29.570	0.5803
NAZCA (NZ)	61.544	-109.781	0.6362
SOUTH AMERICA (SA)	-16.290	121.876	0.1465
JUAN DE FUCA (JF)	-22.417	67.203	0.8297
PHILIPPINE (PH)	-43.986	-19.814	0.8389
RIVERA (RI)	22.821	-109.407	1.8032
SCOTIA (SC)	-43.459	123.120	0.0925
NNR*	2.429	93.965	0.2064

After *DeMets et al.* [1994]

*No net rotation, defined in §6.6

Although the table lists only Euler vectors with respect to North America, the motion of plates with respect to other plates is easily using vector arithmetic. For example,

$$\omega_{ij} = -\omega_{ji}, \tag{13}$$

so we reverse the plate pair using the negative of the Euler vector. The pole for the new plate pair is the antipole, with latitude of opposite sign and longitude increased by 180°. The magnitude

(rotation rate) stays the same. We can also reverse the plate pair by keeping the same pole and making the rotation rate negative (clockwise rather than counterclockwise). Although we usually use positive rotation rates, negative ones sometimes help us visualize the motion. For example, the table shows the Pacific-North America pole at about -49°N, 102°E, so the North America-Pacific pole is at about 49°N, (102 + 180 = 282)°E, which is in eastern Canada. Thus about this pole, North America rotates counterclockwise with respect to the Pacific, or the Pacific rotates clockwise with respect to North America, as shown in Figure 4.

For other plate pairs, we assume that the plates are rigid, so all motion occurs at their boundaries. We can then add Euler vectors,

$$\omega_{jk} = \omega_{ji} + \omega_{ik} \tag{14}$$

because the motion of plate j with respect to plate k equals the sum of the motion of plate j with respect to plate i and the motion of plate i with respect to plate k. Thus if we start with a set of vectors all with respect to one plate, e.g. i, we use

$$\omega_{jk} = \omega_{ji} - \omega_{ki} \tag{15}$$

to form any Euler vector needed. These operations are easily done using the Cartesian components (4), as shown in this chapter's problems.

Adding and subtracting Euler vectors is like what we did for linear velocity vectors in section 6.2.3. We can add and subtract linear velocity vectors only in small areas, such a triple junctions between three plates, where the velocities are evaluated at points near each other. In this case, the east-west and north-south directions are the same, so we can add and subtract the east-west and north-south components. However, adding and subtracting Euler vectors is valid for entire plates. To see this, consider two points r_a on the boundary between plates 1 and 2, and r_b on the boundary between plates 2 and 3. The linear velocities at the two points are

$$\mathbf{v}_{12} = \omega_{12} \times \mathbf{r}_a \quad \mathbf{v}_{32} = \omega_{32} \times \mathbf{r}_b \ . \tag{16}$$

If the two points are the same, **r**, then

$$\mathbf{v}_{12} - \mathbf{v}_{32} = (\omega_{12} - \omega_{32}) \times \mathbf{r} = \omega_{13} \times \mathbf{r} \tag{17}$$

Euler vector addition is important because we only have certain types of data for individual boundaries (Fig. 6.3-6). Although spreading centers provide rates from the magnetic anomalies and azimuths from both transform faults and slip vectors, only the direction of motion is directly known at subduction zones. As a result, convergence rates at subduction zones are estimated by global closure, combining data from all plate boundaries. Thus the predicted rate at which the Cocos plate subducts beneath North America, giving rise to large earthquakes in Mexico, depends on the measured rates of Cocos-Pacific spreading on the East Pacific rise and Pacific-North America spreading in the Gulf of California. In some cases, such as relative motion between North and South America, no direct data were used because the boundary location and geometry are unclear, so the relative motion is inferred entirely from closure. Not surprisingly, the motions of plate pairs based on both rate and azimuth data appear to be better known.

Fig. 6.1-5 shows the predicted relative motions at plate boundaries around the world. As we will discuss in Chapter 8, these motions cause earthquakes and determine the geometry of slip in the earthquakes. Thus we can use the plate motions to make inferences about future earthquakes. For example, as we saw in Fig. 6.2-9, even though we do not have seismological observations of large earthquakes along the boundary between the Juan de Fuca and North American plates, the plate motions predict that such earthquakes could result from the subduction of the Juan de Fuca plate beneath North America. Evidence for this subduction is given by the presence of the Cascade volcanoes (such as Mount Saint Helens and Mount Rainier) and geologic records showing evidence of large past earthquakes.

We note in section 6.1.1 that boundaries between plates are often diffuse zones. In addition to seismicity, active faulting, and elevated topography, plate motion data provide another method of studying them. many of which are themselves earthquake slip vectors. For example, Fig. 6.1-5 shows zones of seismicity in the Central Indian Ocean as boundaries between distinct Indian and Australian plates, rather than as within a single Indo-Australian plate, because spreading rates along the Central Indian Ocean ridge are better fit by a two-plate model. A similar argument justifies the assumption of a small Rivera plate distinct from the Cocos plate. Another approach is to

use the global plate circuit closures (Fig. 6.3-6). Recall that forming an Euler vector from two others (Eqn 10) assumes that all three plates are rigid. Hence this assumption can be used to test for deviations from rigidity. To do this, we form a *best fitting vector* for a plate pair using only data from that pair of plates' boundary, and a *closure fitting vector* from data elsewhere in the world. If the plates were rigid, the two vectors would be the same. However, a significant difference between the two indicates a deviation from rigidity, or another problem with the plate motion model.

A variant on this approach is to examine the Euler vectors for three plates that meet at a triple junction, compute best fitting Euler vectors for each of the three plate pairs, and sum them. For rigid plates, Eqn 14 shows that the sum should be zero. This procedure is analogous to the way the linear velocities should sum to zero (section 6.2.3). However, when this was done for the junction in the Central Indian Ocean, assuming that it was where the African, Indo-Australian, and Antarctic plates met, the Euler vector sum differed significantly from zero, indicating deviations from plate rigidity. As plate motion data improve, it seems that what was treated as a three-plate system may include as many as six resolvable plates (Antarctica, distinct Nubia (West Africa) and Somalia (East Africa), India, Australia, and Capricorn (between India and Arabia)).

6.4 SPACE GEODESY

6.4.1 Motivation

As we have seen, plates move very slowly, a few centimeters per year. Measuring such slow motions is a challenge. Until recently this could only done by measuring the relative displacement of features such as magnetic isochrons or stream beds that had accumulated over long periods of time and could be dated. Dividing the offset distance by the time gives the average rate of motion. For example, motion between the Pacific and North American plates along the San Andreas fault has offset the stream called Wallace Creek[1] by 130 m (Figure 1). Radiometric dating of charcoal (section 5.5.3) in the stream bed shows that this occurred over the past 3700 years. Thus the plate motion here is 130 m / 3700 years, or 34 mm/yr.

Although such measurements are extremely valuable, they have two limitations. First, they can only be made at places where dated features are offset. Second, they give the average motion over long periods of time. However, we would like to measure plate motions at many places and over short periods of time, to see how they compare to the average rates.

Alfred Wegener suggested doing this when he proposed the theory of continental drift in 1915. To test his theory that continents had drifted apart over hundreds of millions of years, he tried to measure the changing distance between continents. Such measurements involve geodesy, the science of measuring the shape of the earth and distances on it. For scientific purposes, we use very high precision versions of the techniques used by surveyors to measure positions to establish land ownership, locate roads, and other applications.

Most geodetic techniques rely on detecting the motion of geodetic monuments, which are markers in the ground. The most familiar monuments are the metal disks attached to rocks often seen at mountain peaks. In soft sediment, monuments are often steel rods driven deep into the earth. Although the popular term for monuments is "benchmarks," geodesists reserve this term for monuments used to study vertical motions.

[1] Named after geologist Robert Wallace, who first made these measurements here.

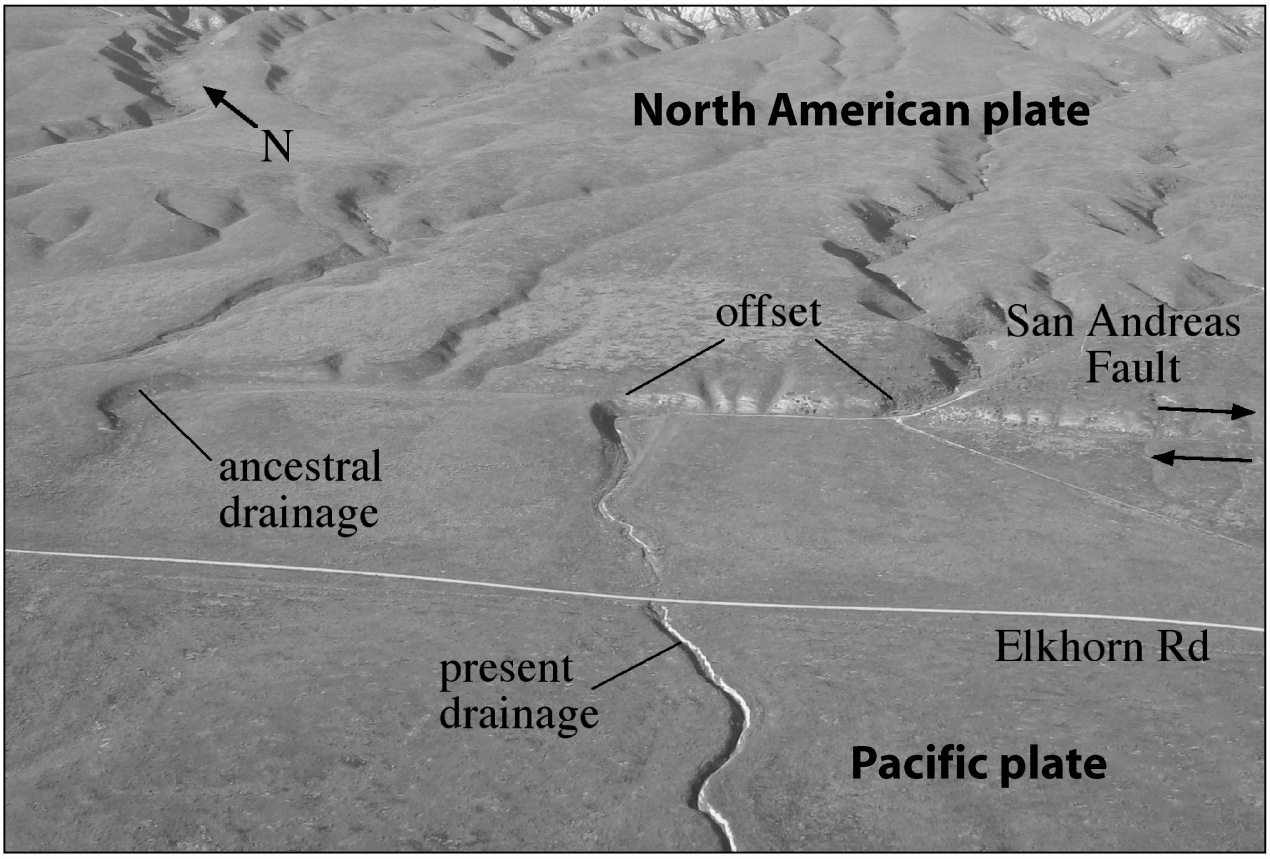

Figure 6.4-1: Wallace Creek, on the San Andreas fault. The 34 mm/yr rate of motion across the fault, and thus between the Pacific and North American plates, is measured here using the offset of stream channels resulting from motion across the fault. These measurements are confirmed by space geodesy. (USRA)

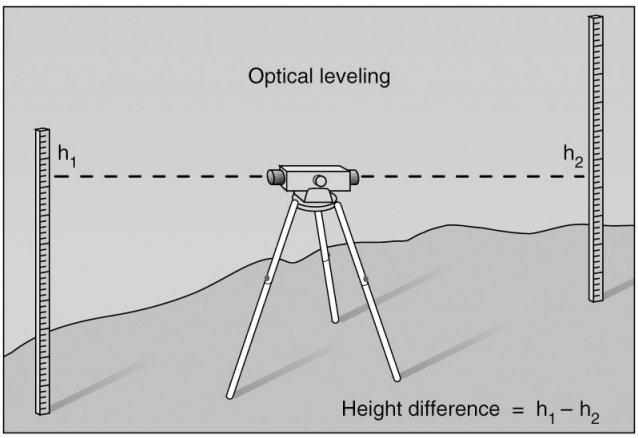

Figure 6.4-2: Measurement of vertical positions using leveling. (Davidson et al., 2002)

Until recently, such measurements were typically made by triangulation, which measures the angles between monuments using a theodelite, or trilateration, which measures distances with a laser. Vertical motion was measured by leveling, using a precise level to sight on a distant measuring rod (Figure 2). However, such surveying methods offered no hope of measuring slow motions between continents, because the continents were too far apart for measurements to be made between them.

To get around this problem, Wegener tried using astronomical observations. Instead of measuring positions on either side of the Atlantic relative to each other, he tried to measure how their positions were changing relative to stars. This idea - measuring motions relative to something in space - is now called space geodesy. It has a long history. In about 230 BC Eratosthenes found the Earth's size from observations of the sun's position at different sites (section 2.2) and navigators have found their positions by observing the sun and stars. However, because measuring continental drift required detecting small changes in positions over a few years, it called for measurement accuracies far greater than possible at the time. Wegener's attempts failed, and the idea of continental drift was largely rejected.

By the 1970's the story was quite different. Geologists accepted continental drift, in large part because paleomagnetic measurements - ones based on the earth's magnetic field recorded in rocks (section 7.2.3) - showed that continents had in fact moved over millions of years. Moreover, space technology was evolving to the point where it could measure continental motions over a few years.

6.4.2 Methods

Space geodesy is one of the most complex technologies used in the earth sciences. It uses electromagnetic waves to locate a geodetic monument in ways analogous to locating an earthquake with seismic waves. One technique, Very Long Baseline Interferometry (VLBI) uses radio signals from quasars, mysterious radio sources that are thought to result from black holes at the center of distant galaxies. Quasars are incredibly energetic, producing more energy than entire galaxies from a volume about the size of the solar system. The signals are recorded by radio telescopes, which are highly sensitive large radio receivers like the one used in the film "Contact" to detect signals from

extraterrestrial life. Radio waves arrive at telescopes separated by long distances - hence "Very Long Baseline" - at different times depending on the difference in the length in their paths to the two telescopes (Figure 3). The time difference is measured very precisely by shifting the signals until their sum is largest. Because the phase of a sine wave oscillates through 360° (Chapter 3), the sum of two waves is maximum when peaks and troughs line up. This condition is called constructive interference or being in phase. Their sum is minimum when they are 180° apart and cancel out, which is called destructive interference or being out of phase. Multiplying the time difference by the speed of light gives the path difference in the direction toward the quasar. Observing many radio sources at different telescopes gives their relative positions to amazing precision. Measuring the positions over time yields the rates and directions of motion between the telescopes and thus plate motions.

These measurements require almost unbelievably precise atomic clocks, that use the fact that atomic transitions emit electromagnetic waves with characteristic frequencies (Chapter 10). For example, sprinkling salt on a flame gives an orange glow due to transitions in sodium. Any process that happens over and over again at a regular speed can be used as a clock. Because the pendulum in a grandfather clock swings back and forth at the same rate, counting swings can be used to keep time. In a atomic clock, transitions of atoms as they move back and forth between two energy levels are counted to keep time. These are so precise that the fundamental unit of time, the second, is defined as the time needed for a number of transitions between two energy levels of the ground state of the cesium-133 atom. The clocks are accurate to a few picoseconds (1 picosecond is a trillionth of a second, or 10^{-12} s), so the positions can be found to precision of about 3×10^{8} m/s $\times\, 3 \times 10^{-12}$ s $\approx 10^{-3}$ s or 1 mm. Because speed is distance divided by time, observations over a period of years can measure plate motions to a precision of millimeters per year.

The technique of interferometry, measuring times and differences very precisely from the phase differences between two waves, is used widely in space geodesy and many other applications. As we saw in Chapter 4, crystal structure is found using X-ray diffraction, in which interference between X-rays gives the spacing between crystal planes. The Michelson-Morley experiment in 1887, one of the most famous experiments in physics, used interferometry to show that the speed of

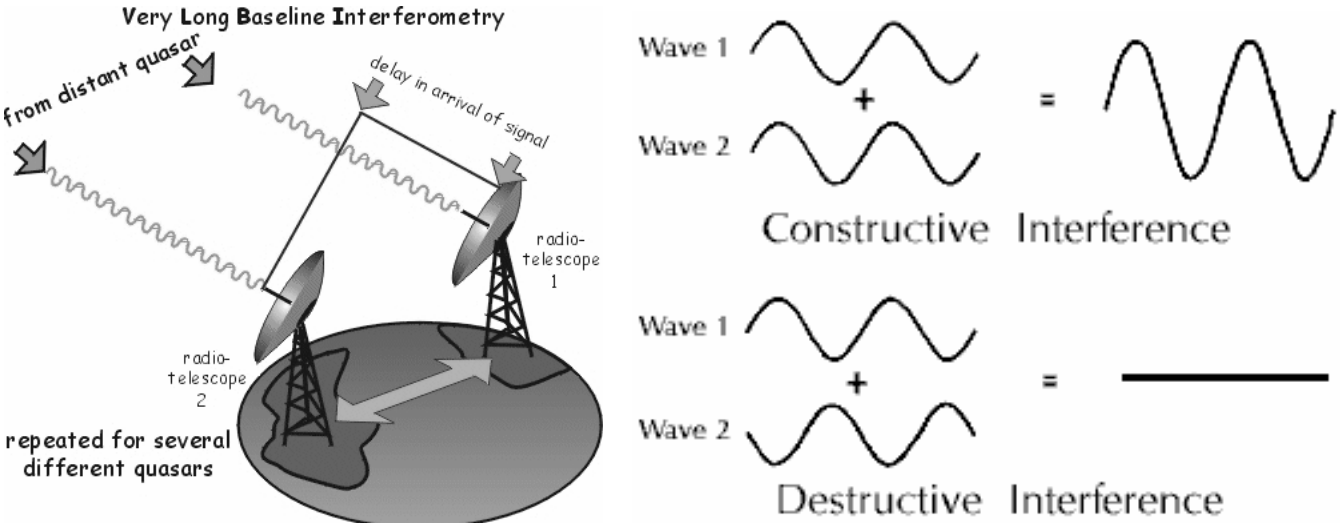

Figure 6.4-3: *Left:* Very Long Baseline Interferometry (VLBI) uses the difference in the times radio waves from quasars arrive at two telescopes to measure the distance between them. (www.leeds.ac.uk/../active_tectonics/vlbi.gif) *Right:* The time difference is measured by interferometry, that uses the phase difference between the signals.

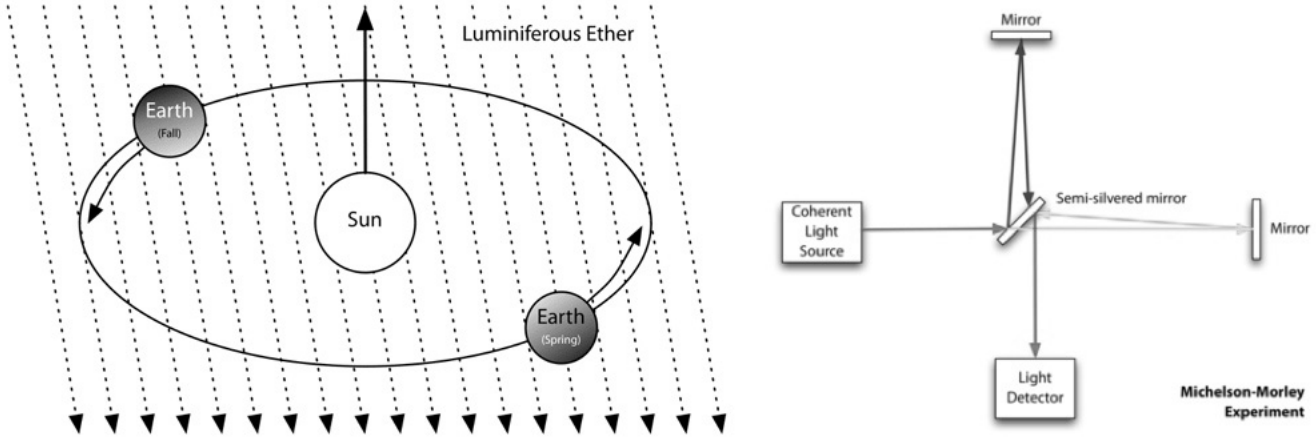

Figure 6.4-4: Interferometry was used to show that the speed of light was the same in all directions in the Michelson-Morley experiment. (Wikipedia)

light was the same in all directions (Figure 4). This disproved the theory that light propagated in the "luminiferous ether" that was hypothesized to fill interplanetary space, because in that case the speed would vary from day to night or between seasons depending on how the light moved relative to the ether. Discarding the ether idea led in 1905 to Einstein's theory of special relativity, which assumes that all observers measure the speed of light to be the same no matter what their linear motion is.

A second technique, Satellite Laser Ranging (SLR), uses the time required by light from ground lasers to bounce off satellites (Figure 5). Repeated measurements give both the satellites' orbits and the positions of the ground stations as a function of time. The satellites are covered with special corner reflectors that reflect very well because by Snell's law the ray reflected twice is parallel to the incident ray. A similar technique has been used to study the moon's orbit, using reflectors installed by the Apollo missions. Often corner reflectors are used when we want to be seen, as on bicycles and boats. Conversely, corners that could act as reflectors are avoided when we don't want to be seen, as in radar-avoiding stealth aircraft that are designed with smooth surfaces (Figure 6).

Although VLBI and SLR yield excellent data, the observing systems are expensive, heavy, and hard to move to remote locations. Hence most plate motion measurements are made using the Global Positioning System (GPS)[2] or similar systems using the travel time of radio signals between satellites and receivers on the ground. These have the advantage that much of the complexity of the system is in the satellites, making the receivers much less expensive and easier to transport.

GPS was developed in the late 1970's by the U.S. Department of Defense for real-time positioning and navigation. A constellation of satellites orbit the earth, so at least four are overhead most of the time anywhere in the world. They transmit radio signals that are recorded by receivers on the ground and used to find the receivers' position from the time the signals arrive (Figure 7). The process of finding a position with radio signals from different satellites is like locating an earthquake from arrivals at multiple seismometers (Chapter 3). GPS positions are 2-3 times more precise in the

[2] Space geodesy grew up in the world of space and military technology, so there are lots of acronyms. In addition to their official meanings there are unofficial alternatives. Because of the many people needed, VLBI is said to be "Very Large Bunch of Investigators." Since GPS receivers are set up to record data for hours while investigators hang around, people have suggested "Great Places to Sleep." There are also second-level acronyms involving other acronyms, such as IGS for International GPS Service. A mark of true space technology gurus is using third-level acronyms.

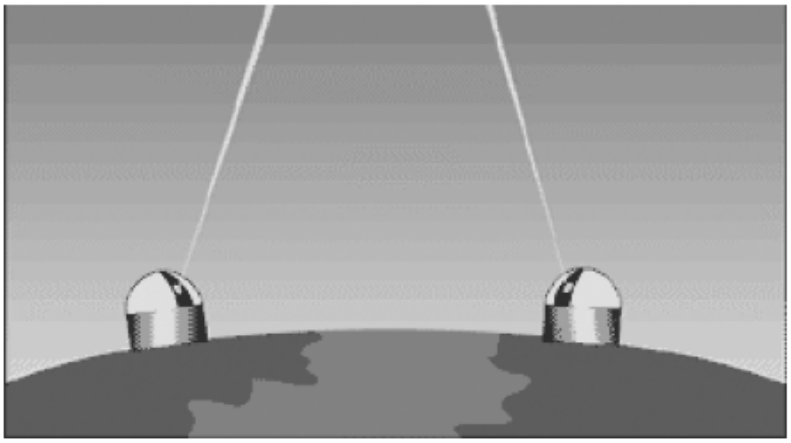

Figure 6.4-5: Satellite Laser Ranging (SLR), uses the time required by light from ground lasers to bounce off satellites. (NASA)

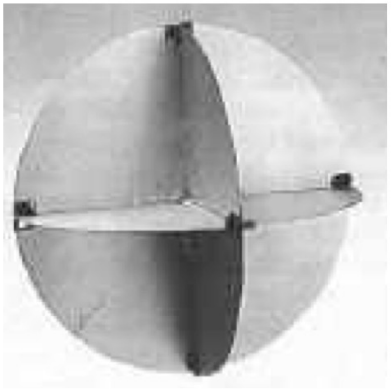

Figure 6.4-6: Rays reflected from a corner reflector emerge parallel to the incident ray *(left)*. (Wikipedia) *Top right:* A metallic reflector with corners used on boats to make them more visible to radar. *Bottom right:* Aircraft built to be difficult to detect with radar have as few corners as possible.

horizontal than vertical, because signals arrive only from above, just as earthquake locations are less precise in depth because seismic waves arrive only from below.

Using GPS for tectonics is an extension of the way GPS is used by drivers, boaters, and hikers. The satellites transmit signals that contain navigation data that identifies the satellite and describes its orbit, and a coded timing signal containing the time from an atomic clock. These signals are used to adjust, or modulate, much higher frequency "carrier" signals. This operation is similar to the way radio stations transmit music by modulating the amplitude (AM) or frequency (FM) of carrier waves, whose frequency is the setting on a radio dial. Just as a radio extracts music from the carrier, GPS receivers extract the timing and navigation signals. The receiver compares the timing signal arriving from a satellite to one it generates, and finds the time difference. Multiplying the time difference by the speed of light gives the distance, or pseudorange, between the receiver and the satellite. The term "pseudorange" is used because during the time the signal takes to reach the receiver the satellite has moved. From the pseudoranges to a minimum of four satellites and the satellite orbit information, a small inexpensive GPS receiver can determine its 3-dimensional position to a precision of a few meters (Figure 8).

The improvement to mm-level or better precision is obtained using more expensive GPS receivers and comparing the carrier signals to a carrier generated in the receiver. Because the carriers have higher frequencies and thus shorter wavelengths than the modulations, using their phase can yield more precise locations. The carrier wavelengths are 19 and 24 cm, so precise phase measurements can resolve positions to a fraction of these wavelengths. A number of other methods improve the precision even more. Combining signals from multiple satellites recorded at multiple receivers reduces the effect of uncertainties in the clocks in the satellites and receivers. Combining both carrier frequencies removes the effects of the passage of the radio signals through the ionosphere, the upper layer of the atmosphere that is ionized by radiation from the sun. Position errors that result from the radio signals being delayed by water vapor in the lower atmosphere can be reduced by solving for the delays using methods like those used to find seismic velocity structure.

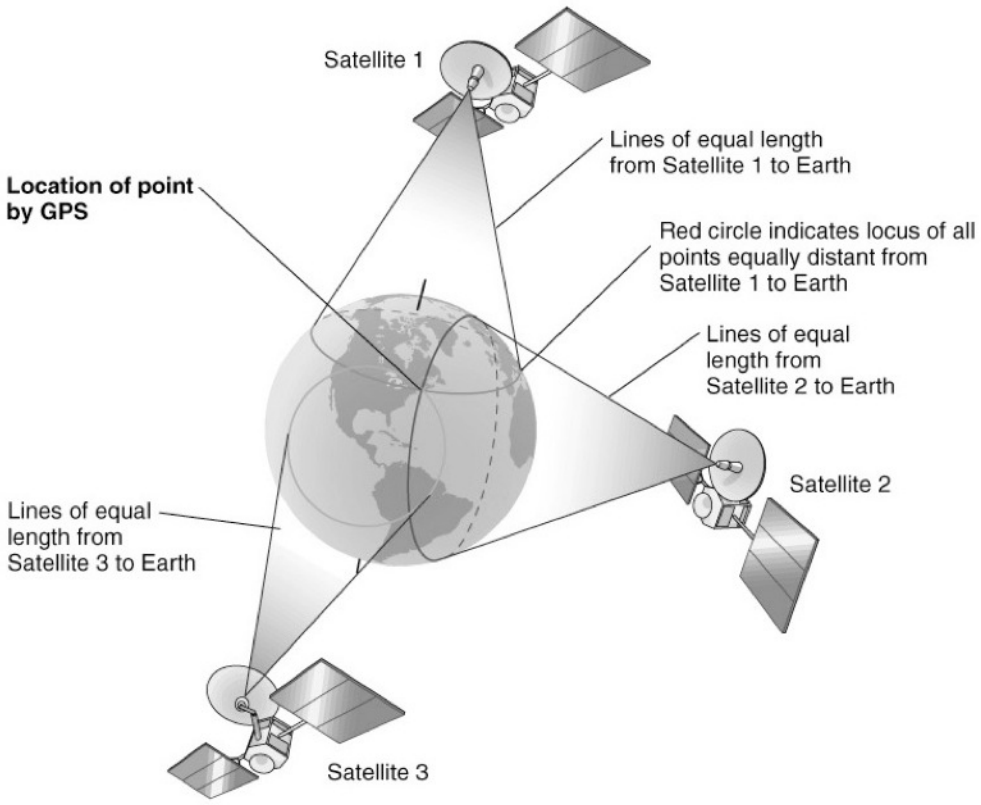

Figure 6.4-7: Use of GPS satellites to locate a receiver. (Davidson et al., 2002)

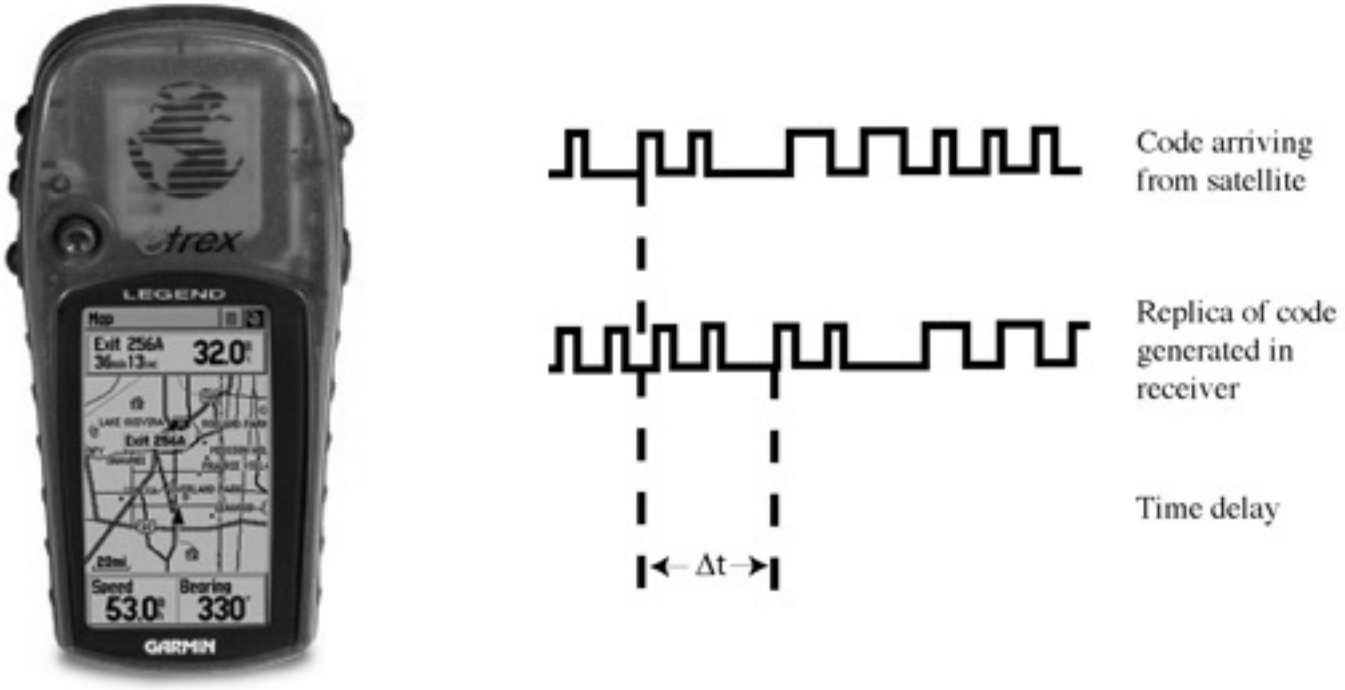

Figure 6.4-8: An inexpensive GPS receiver finds the time taken by the signal to arrive from each satellite by comparing it to one generated in the receiver.

The final element for high-precision surveys is provided by continuously operating global GPS tracking stations and data centers. These provide high-precision satellite orbit and clock information and a global reference frame. Using this information GPS studies can measure positions to a few mm, so measurements over time yield relative velocities to precisions of a few mm/yr or better, even for sites thousands of kilometers apart.

GPS data are collected in two ways (Figure 9). In survey mode, GPS antennas are set up over monuments for short periods, and the sites are reoccupied later. Alternatively, continuously recording GPS receivers are permanently installed. Continuous GPS provides significantly more precise data at higher cost. For plate motion studies either works well, but continuous data are better. As a result, global plate motion models from space geodetic data primarily use the velocities of continuous sites to find Euler vectors. Continuous data also have the advantage that they can detect transient motions over short times, such as those after a major earthquake, that making a measurement every few years would miss.

6.4.3 Precision and Accuracy

The challenge for space geodesy is to measure positions so well that their slow motions can be detected in a few years. This is like using a scale every morning to see if a diet is working. The scale should be both precise and accurate. The precision, how repeatable the weight you get from stepping on the scale several times, controls how long it takes to see if you're losing weight. If the scale is only precise to a pound, it may take several weeks to tell if the diet's working. A less precise scale means you would need longer. The scale should also be accurate, in that it gives your true weight. If the scale gives too-high values, you may not need to be on a diet at all.

This example shows why although we talk of "measuring" quantities, a statistician would say that we're really "estimating" them. That's because the number we get is derived by combining measurements under certain assumptions. The uncertainty in the estimate comes from both random and systematic errors. We describe the part of the uncertainty coming from random errors by the precision, which measures the uncertainty resulting from the measurement system. This involves both the

Figure 6.4-9: *Left:* In survey mode, a GPS antenna is set up over a geodetic marker. *Right:* A permanent GPS site. The antenna is under the protective dome and the solar panel provides power in this remote location.

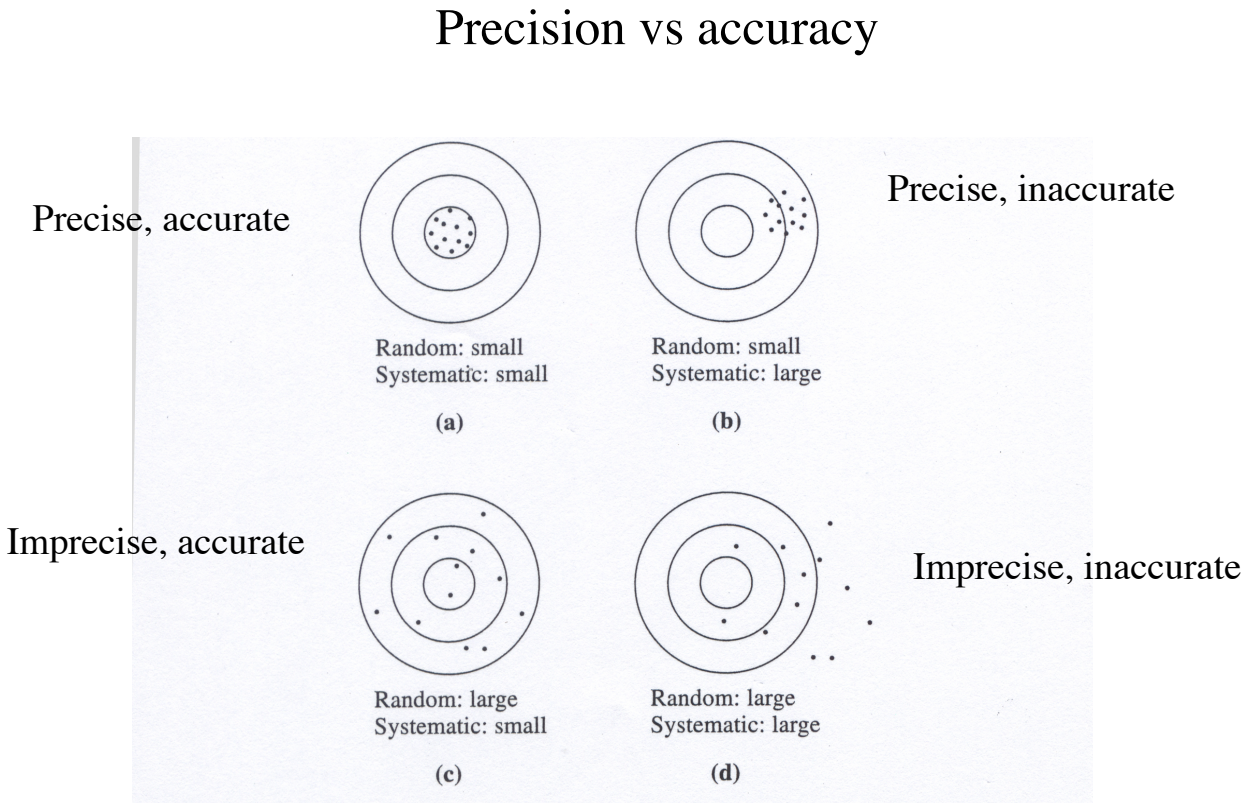

Figure 6.4-10: Illustration of the concepts of precision and accuracy (Taylor, 1997)

equipment and how it is used. In the diet example, some uncertainty is intrinsic to the scale, and some results from how carefully you use it. You'd get different answers with and without shoes on. To assess the precision, you would weigh yourself several times and estimate the precision from how the results scatter around the average.

We describe the other part of the uncertainty coming from systematic errors by the accuracy. Ideally, we calibrate our measurements by comparing our results to a known standard. However, often we don't have a known value to compare to. In that case, we estimate the accuracy by comparing the results of different measurements. Thus to see how accurate our scale is, the best thing would be to weigh the international standard kilogram, a cylinder of platinum and iridium kept in a locked safe near Paris[3]. Because this isn't practical, we could weigh some objects whose weight we think we know. If we didn't have any, we could weigh ourselves on several scales and estimate the accuracy from how the results scatter around the average.

As this example shows, we can have measurements that are precise but not accurate, or accurate but not precise. Getting on a precise but miscalibrated scale several times will give very similar but inaccurate weights. Comparing several accurate but imprecise scales will yield a good average weight with a lot of scatter. Another way to see this is to compare results from shooting a gun at a target (Figure 10). If the shots cluster tightly, the random errors are small, so precision is high. If they cluster around the target's center, the systematic error is small, so accuracy is high. Although ideally the shooting is precise and accurate, we can have different combinations. The trick is that in the real world we don't know where the target is - we're trying to figure that out from the measurements. Thus it's easy to assess the precision of the measurements, but hard to assess their accuracy.

Because it's easier to address, we usually focus first on the precision of measurements. Figure 11 shows the results of 50 measurements of the positions of two sites on the Northwestern campus using simple GPS receivers. For each site, we take the usual approach of describing the N measurements x_i by their average, or *mean*

[3] Remember that a kilogram is a unit of mass, not weight.

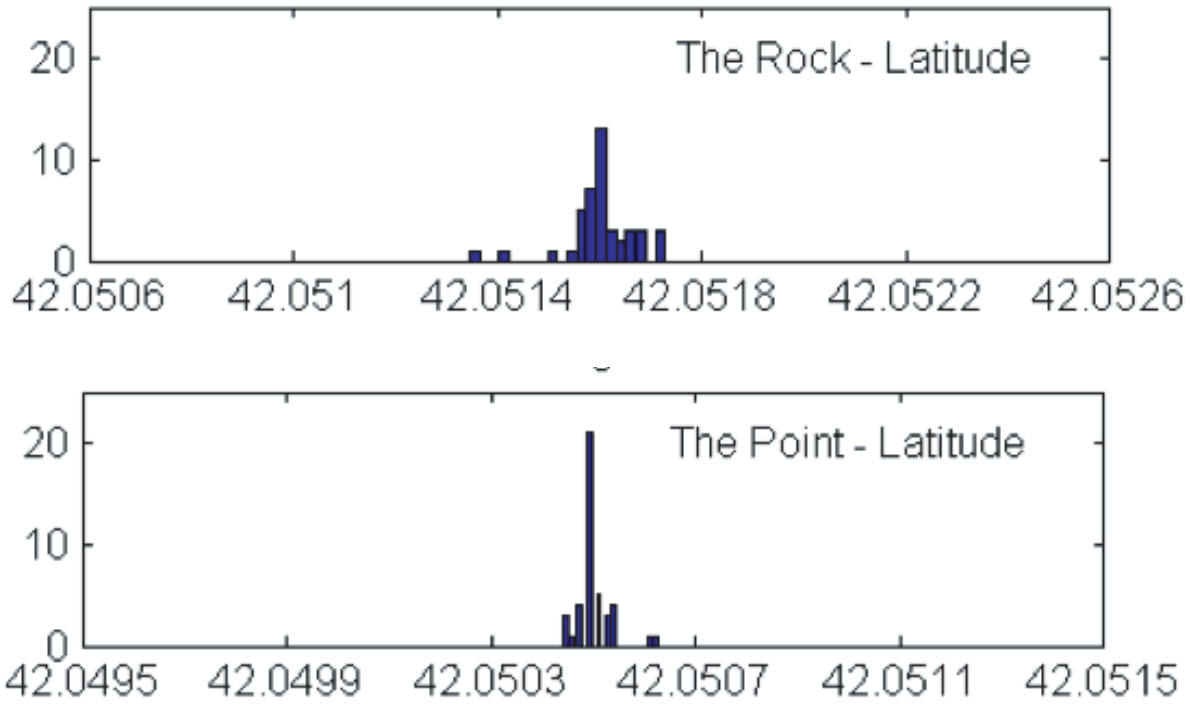

Figure 6.4-11: Histograms comparing the latitudes found in 50 GPS measurements of the positions of two sites on the Northwestern campus.

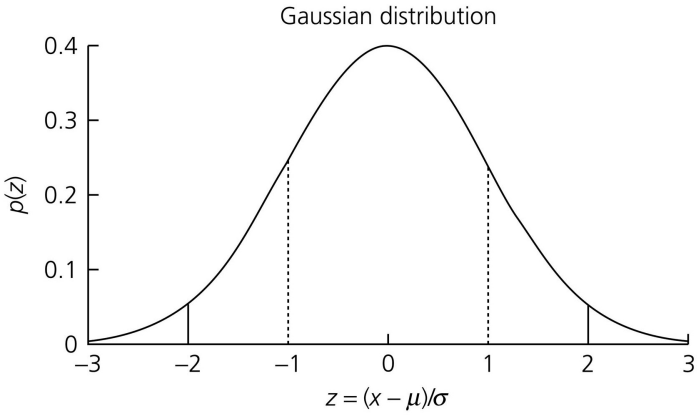

Figure 6.4-12: Probability density function for a Gaussian distribution with mean μ and standard deviation σ. Ranges within one and two standard deviations of the mean are shown by vertical lines.

$$\mu = \left[\frac{1}{N} \sum_{i=1}^{N} x_i \right], \tag{1}$$

and their spread about the mean, or *variance*

$$\sigma^2 = \left[\frac{1}{N} \sum_{i=1}^{N} (x_i - \mu)^2 \right]. \tag{2}$$

σ is called the standard deviation of the distribution. The histograms of the number of measurements with values in a certain range show a peak near the mean and smaller numbers on either side.

Because the data at the "Rock" are more scattered than those at the "Point," they have a larger standard deviation. This occurs because the "Rock" is surrounded by buildings that interfere with the satellite's radio signals, whereas the "Point" is in an open area on the shore of Lake Michigan. The two sites' average standard deviation is 0.000055 degrees, so multiplying by the 111 km in a degree shows that the standard deviation is 6 meters. This is the precision of these measurements.

In geodesy, we often are trying to decide whether a site is moving, and if so, how fast. This requires deciding whether the change in the site's position from an earlier time is large enough to make it likely that it moved. To answer this, we turn the question around by comparing the apparent motion to the uncertainty in the previous position and asking how likely is it that the change is not real. In other words, how likely is it that we would see an apparent change even if the site were not moving, simply because of the uncertainty in the site's position?

To address this question, we use concepts from probability and statistics. We first assume that the values we measured are random samples from a "parent distribution" described by the probability density function $p(x)$ that gives the probability of observing a certain value. Because the measured values are spread about evenly on either side of the mean, we assume that the parent distribution is a Gaussian distribution. This distribution is also called the "normal distribution" because it many different sets of data ranging from earthquake travel time to IQ test scores.

For a Gaussian distribution, the probability that the i^{th} measurement would yield a value in the interval $x_i \pm dx$, in the limit as $dx \rightarrow 0$ is

$$p(x_i) = \frac{1}{\sigma\sqrt{2\pi}} \exp\left[\frac{-1}{2}\left(\frac{x_i - \mu}{\sigma}\right)^2\right]. \quad (3)$$

The distribution thus is characterized by two parameters, the mean μ and the standard deviation σ. The most probable measurement is the mean value, and values on either side of it are less likely the further from the mean they are. The distribution is often written as a function of the normalized variable $z = (x - \mu)/\sigma$,

$$p(z) = \frac{1}{\sqrt{2\pi}} \exp[-z^2/2]. \quad (4)$$

Figure 12 shows the familiar "bell curve" that results.

Because of the uncertainties, the measurements scatter around the mean. Although we can't predict the value of a given measurement, we can estimate how likely it is to be within a range z from the mean. To do this, we integrate the probability density function to find the cumulative probability

$$A(z) = \int_{-z}^{z} p(y)dy = \frac{1}{\sqrt{2\pi}} \int_{-z}^{z} \exp[-y^2/2]dy. \quad (5)$$

For $z = 1$, we get $A(z) = 0.68$, indicating that there is a 68% probability that a measurement will be within one standard deviation of the mean, or between $x - \sigma$ and $x + \sigma$. Conversely, there is a 32% probability that it will be outside this range. Thus if we have a set of measurements, one-third or 32% will appear different from the mean at 68% confidence, purely by chance. Similarly, $A(2) = 0.95$, indicating a 95% probability that a measurement will be within two standard deviations of the mean, or a 5% probability that it will be outside this range. $A(3) = 0.997$, so there is greater than a 99% probability that a measurement will be within three standard deviations.

This concept is important in geodetic studies or any other experimental science. It shows that we have to be careful not to overinterpret results. For any given site, we can't say with confidence that a site has moved unless the new position differs by at least two standard deviations from an earlier one. There may have been some motion, but we can't be confident that there was. Moreover, if we measure the positions of sites that haven't actually moved at all, 32% will appear to have moved at 68% confidence, and 5% will appear to have moved at 95% confidence.

We can extend this analysis to figure out how the uncertainty in the site's position maps into the uncertainty in its velocity. A useful result called the propagation of errors says that if v is a function of two variables x and y that vary independently

$$\mathrm{v} = f(x, y), \tag{6}$$

then its variance is related to the variances of x and y by

$$\sigma_{\mathrm{v}}^2 = \sigma_x^2\left(\frac{\partial \mathrm{v}}{\partial x}\right)^2 + \sigma_{\mathrm{y}}^2\left(\frac{\partial \mathrm{v}}{\partial y}\right)^2 . \tag{7}$$

The amount that each variable contributes to the uncertainty in the function depends on the partial derivative of the function with respect to that variable.

Thus the rate v of motion of a monument that started at position x and reaches y in time T is

$$\mathrm{v} = (y - x)/T. \tag{8}$$

If the uncertainty in each position is given by σ, the resulting uncertainty in the rate is

$$\sigma_{\mathrm{v}} = 2^{1/2}\sigma/T. \tag{9}$$

This equation shows that how precisely we can measure a site's motion depends on how precisely we measure its position at different times and the length of time between the measurements. The three components of the site velocity are found by fitting a least squares line to the positions as a function of time (Figure 13). The precision of a rate measurement improves by taking a longer time interval, even if the positions do not become more precise. Graphically (Figure 14) this is because the rate is the slope of a line, so measurements further apart give a more precise slope. An important consequence of this result is that older geodetic data, for example those taken shortly after the 1906 San Francisco earthquake, can be of great value even if their errors are larger than those of more modern data.

Geodesy usually deals with vector quantities: positions, velocities, or Euler vectors. Each component has an uncertainty so the vector's uncertainty is a three dimensional ellipsoid. To visualize this, we typically plot the uncertainties in the horizontal components as an ellipse.

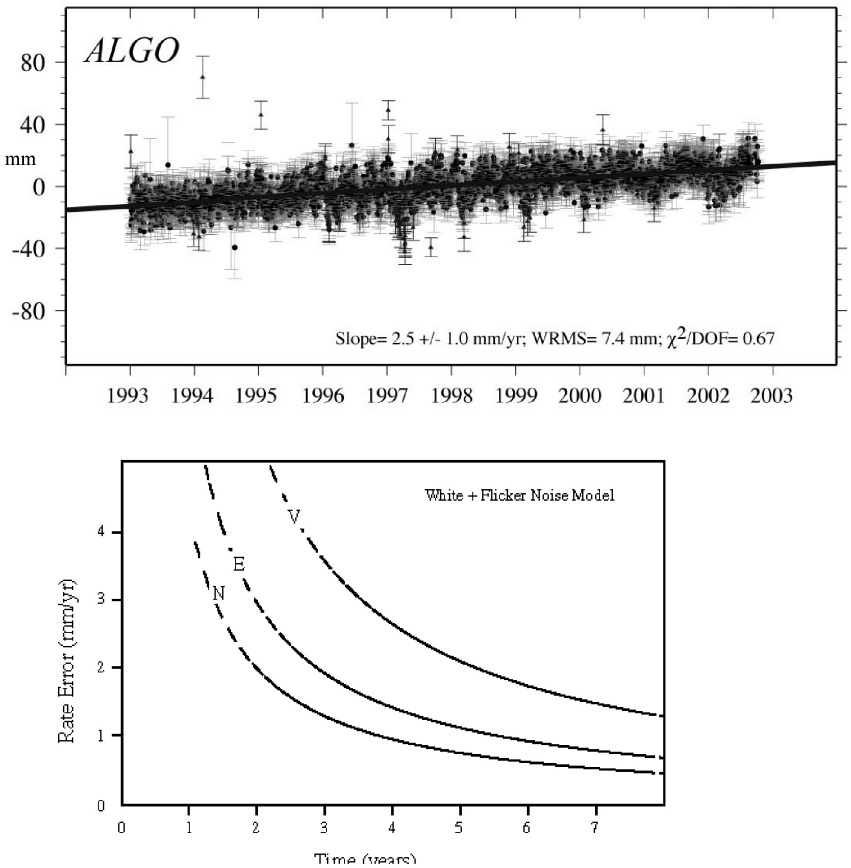

Figure 6.4-13: *Top:* The velocity of a space geodetic site is found from the slope of its position over time. *Bottom:* The precision of the rate estimate increases with length of time over which it is measured, as shown by the decreasing error. The vertical positions are the most uncertain. Because the satellites' orbits are closer to north-south, the north-south rates are more precise than east-west ones. (Sella et al., 1993)

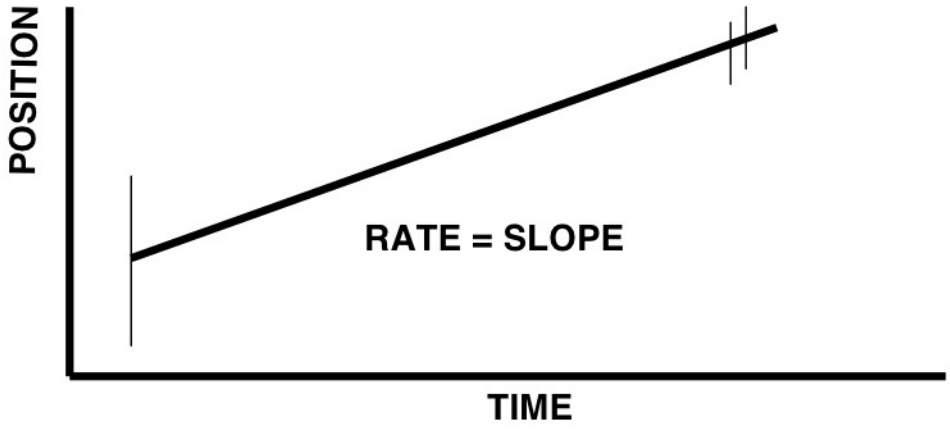

Figure 6.4-14: The precision of a rate estimate can be improved by using older data even if they are less precise than newer data, because the older data lengthen the duration of measurements.

6.4.4 Results

Space geodesy measures both the rate and azimuth of the motions between sites, and can thus be used to compute relative plate motions. This lets us see geological processes happening over a few years rather than waiting millions of years. Seeing geology taking place on human timescales is a very powerful tool.

Space geodetic results are shown in several ways. Figure 15 shows how a line from Massachusetts to Germany measured by VLBI has been lengthening over the years. Although there is some scatter and a yearly variation due to the seasons, the slope clearly shows the opening of the North Atlantic. How in detail this occurs is shown by the motion of GPS sites in Iceland, through which the Mid-Atlantic Ridge passes. The vectors show site motion velocities with respect to the west coast, which is on the North American plate. The ellipses at the end of each vector show the 95% confidence limits on the horizontal velocity. If the vectors were inside the ellipses, there would be a 95% chance that they did not show any motion. The sites are clearly moving because the velocity vectors are well outside the ellipses. The vectors and their projection on a cross section show that extension is occurring on both the east and west rift zones that make up the Ridge. Thus over 200 km, the full opening between the North American and Eurasia plates, about 20 mm/yr, occurs. This rate, measured over a few years, is consistent with the average North Atlantic opening rate measured from magnetic anomalies over 80 million years (Section 6.3.4).

One of the most important results of space geodesy for seismology is that plate motions have remained about the same for the past few million years. This is shown by the striking agreement between motions measured over a few years by space geodesy and the predictions of global plate motion models that average over the past few million years (Figure 16). The agreement gives us confidence in both types of data, and interesting insight into how the earth works. It shows that although motion at plate boundaries can be "jerky," as in large earthquakes, the viscous asthenosphere damps out the transient motions and causes steady motion between plate interiors. This is like the way a shock absorber damps out a car’s bouncing as it goes over bumps in the road.

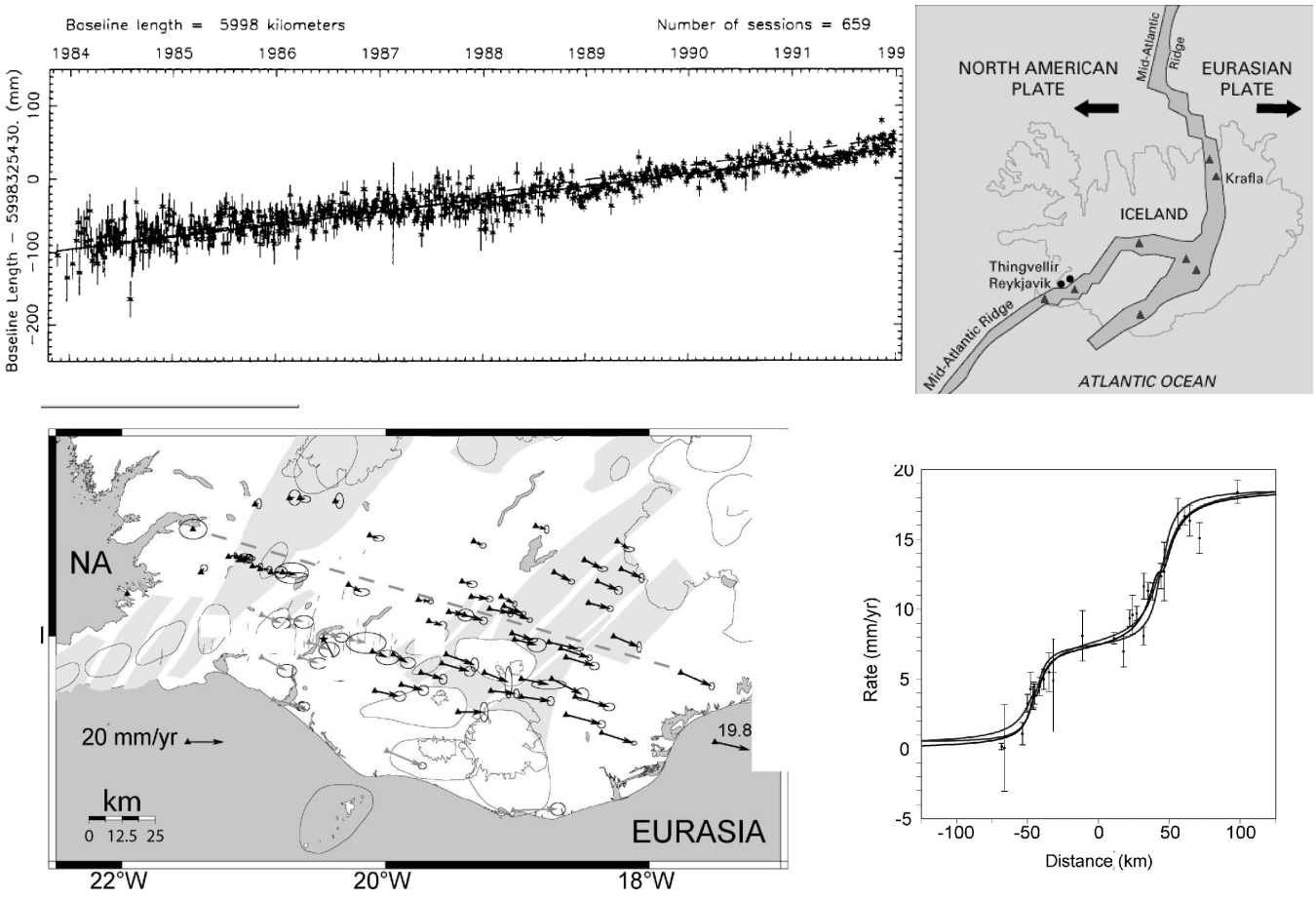

Figure 6.4-15: Space geodetic data showing the opening of the Atlantic. *Top left:* VLBI data showing lengthening of a line from Westford, Massachusetts to Wettzell, Germany. (Ryan et al., 1993) *Lower left:* GPS site velocities showing motions across Iceland, which straddles the Mid-Atlantic Ridge. *Lower right:* GPS site velocities plotted along a profile in the spreading direction. (Lafemina et al., 2005)

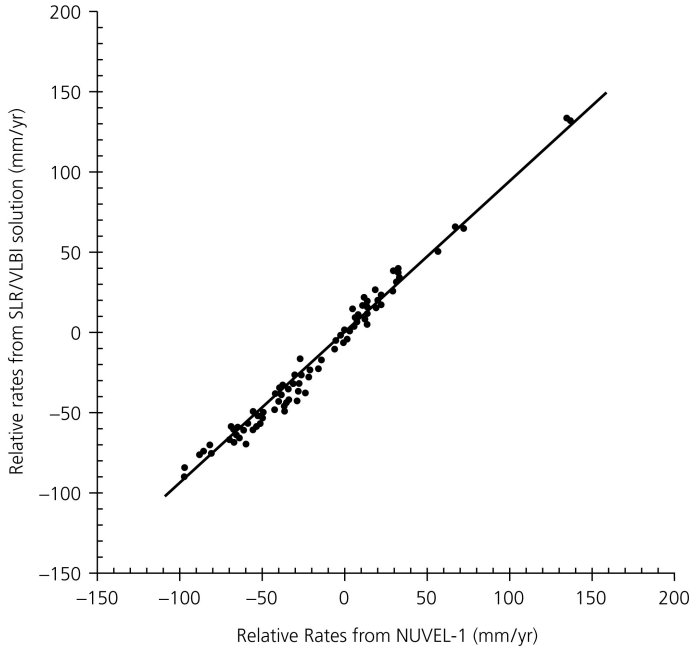

Figure 6.4-16: Comparison of rates determined by space geodesy with those predicted by the NUVEL-1 global plate motion model. The space geodetic rates are determined from sites located away from plate boundaries to reduce the effects of deformation near the boundaries. The slope of the line is 0.94, indicating that plate motions over a decade are very similar to those predicted by a model averaging over 3 million years. (Robbins et al., 1993)

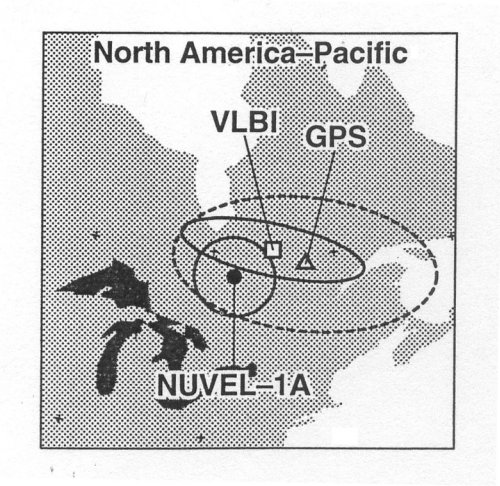

Figure 6.4-17: Comparison of Euler poles for the motion between the Pacific and North American plates. GPS and VLBI poles are derived from space geodetic data, whereas the NUVEL-1a pole comes from geological data. (Argus and Heflin, 1995).

In some places we can see differences between the average motions over the past few million years and those over a few years.The data are good enough that we think we're seeing plate motions changing. Figure 17 shows the Euler pole positions for motion between the North American and Pacific plates from two space geodetic techniques, GPS and VLBI. The poles are similar, and each lies within the other's ellipse of 95% uncertainty, so we can regard them as about the same. The fact that the two techniques agree is nice, because although both use radio signals the method of finding the positions has important differences because GPS signals come from satellites and VLBI's come from quasars. In contrast, the pole from the NUVEL-1 model derived from data that averages motion over the past three million years is somewhat different, though close to the space geodetic ones. In addition, the rotation rate for the space geodetic Euler vectors is a few percent faster. These differences occur because during the past five million years seafloor spreading began in the Gulf of California (Fig. 6.2-10). This rifting transferred Baja California from the North American plate to the Pacific plate. However, this transfer didn't occur instantaneously, but took some time. Thus the average rate of motion recorded by the magnetic anomalies from the Gulf of California is less than the motion today that the space geodetic data measure. GPS sites in Baja show that there is still some motion between Baja and the rest of the Pacific plate, so the transfer isn't completely finished,

In addition to measuring motions taking place today, space geodesy surmounts a major difficulty faced by models like NUVEL-1A. In the geologically based models, the data (spreading rates, transform azimuths, and slip vectors) used to calculate Euler vectors between plates are on their boundaries, so the Euler vector provides only the net motion across a boundary between two plates that are assumed to be rigid. In contrast, space geodesy also measure the motion of sites within plate boundary zones. For example, Figure 18 shows the motions of GPS and VLBI sites within the North America-Pacific boundary zone. Sites in eastern North America move so slowly - less than 2 mm/yr - with respect to each other that their motion vectors cannot be seen on this scale. These sites thus define a rigid reference frame for the stable interior of the North American plate. The site vectors show that most of the plate motion occurs along the San Andreas fault system, but significant motions occur for some distance eastward. The sites directly across the San Andreas move at the rate

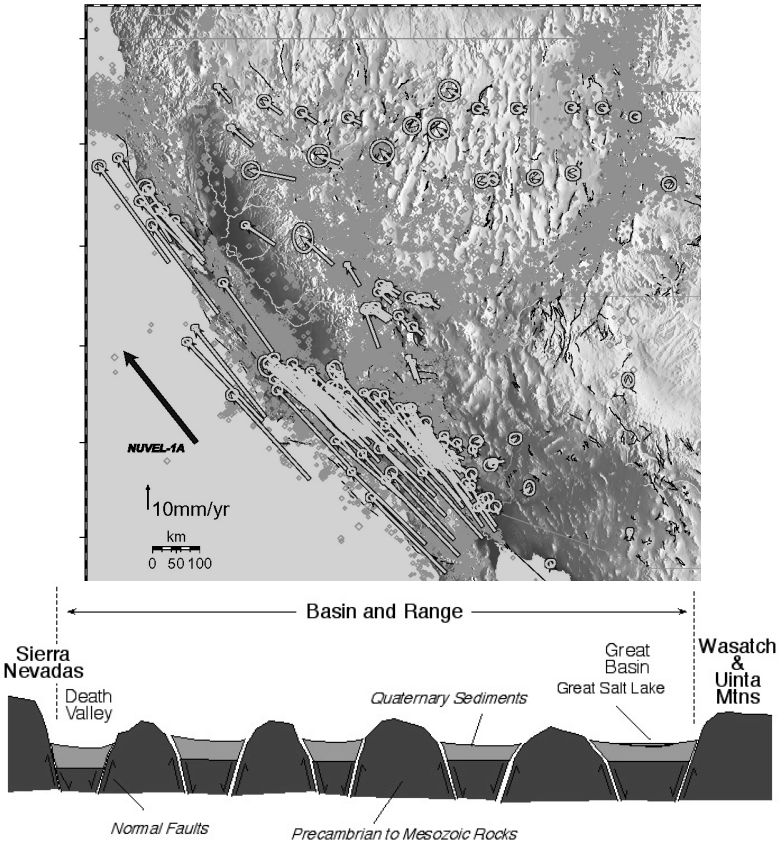

Figure 6.4.18: *Top:* Velocities of space geodetic sites across part of the Pacific-North America boundary zone relative to stable North America. (Bennett et al., 1999) *Bottom:* Schematic geologic cross section of the Basin and Range. (www.gly.uga.edu/railsback)

measured geologically (Figure 1), whereas the overall motion across the boundary zone is that predicted by a global plate motion model derived from space geodetic data (Figure 6.3.4). Within the boundary zone, the site motions show the extension across the Basin and Range province that gives rise to north-south trending topography and faults. The geodetic motions thus are consistent with both the plate motions over the past few million years, with geological data, and the motions that occur in earthquakes. Hence, as we discuss in Chapter 8, the different data types are used together to study how the seismic and aseismic portions of the deformation vary in space and time in the diffuse deformation zones that characterize many plate boundaries. This is done both on large scales, as shown here, and for studies of smaller areas and individual earthquakes.

Space geodesy is also used to study the relatively rare, but sometimes large, earthquakes within plates. Global plate motion models give no idea where or how often intraplate earthquakes should occur, beyond the trivial prediction that they should not occur because there is no deformation within ideal rigid plates. Space geodesy is being combined with earthquake locations, focal mechanisms, and other geological and geophysical data to investigate the motions and stresses within plates and how they give rise to intraplate earthquakes. For example, GPS lets us measure the effects of post-glacial rebound that is one of the possible causes of intraplate earthquakes (Figure 5.4.9).

6.5 FINITE ROTATIONS

6.5.1 Formulation

So far, we have used Euler vectors to describe plate motions today or over the past few million years. On geological time scales, these are "instantaneous" motions described by small or "infinitesimal" rotations around the Euler pole. We also use Euler vectors to describe how plates move over long periods of time. In this case, the motion of a plate from one position to another on the surface of the earth is described by a finite rotation through a large angle around the Euler pole. Thus instead of computing velocities, we find how positions change over time.

Figure 1 shows the idea for two plates *a* and *b* that rifted apart, forming a new midocean ridge and ocean basin. Points on the opposite coastlines like A and A' or B and B' are now separated. Similarly, magnetic anomalies on the two plates that formed at the new ridge move apart as the ocean continues to open.

To describe this motion, we write a point's position before it rotated as **r**. As in equation 6.3.7, we write the position vector in Cartesian coordinates for a point at latitude λ and longitude μ as

$$\mathbf{r} = (a \cos\lambda \cos\mu,\ a \cos\lambda \sin\mu,\ a \sin\lambda). \tag{1}$$

The rotation is described by a matrix R

$$R(\theta, \phi, \Omega_f) = R(\mathbf{e}, \Omega_f) \tag{2}$$

representing a finite rotation by an angle Ω_f about an Euler pole at latitude θ and longitude ϕ. A unit vector from the center of the earth to the pole is

$$\mathbf{e} = (e_x, e_y, e_z) = (\cos\theta \cos\phi,\ \cos\theta \sin\phi,\ \sin\theta). \tag{3}$$

This is like the Euler vector defined in equation 6.3.8 but defines only the pole, without the rotation rate.

Using this notation, we describe the motion of the point **r** to its new position $\mathbf{r}'$ by

$$\mathbf{r}' = R\mathbf{r}\ . \tag{4}$$

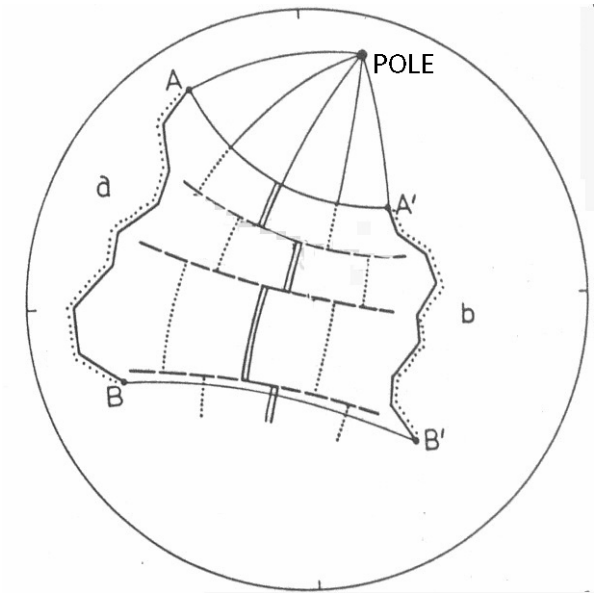

Fig. 6.5.1: Illustration of two plates that separated by a finite rotation about a pole. (Dewey, 1975)

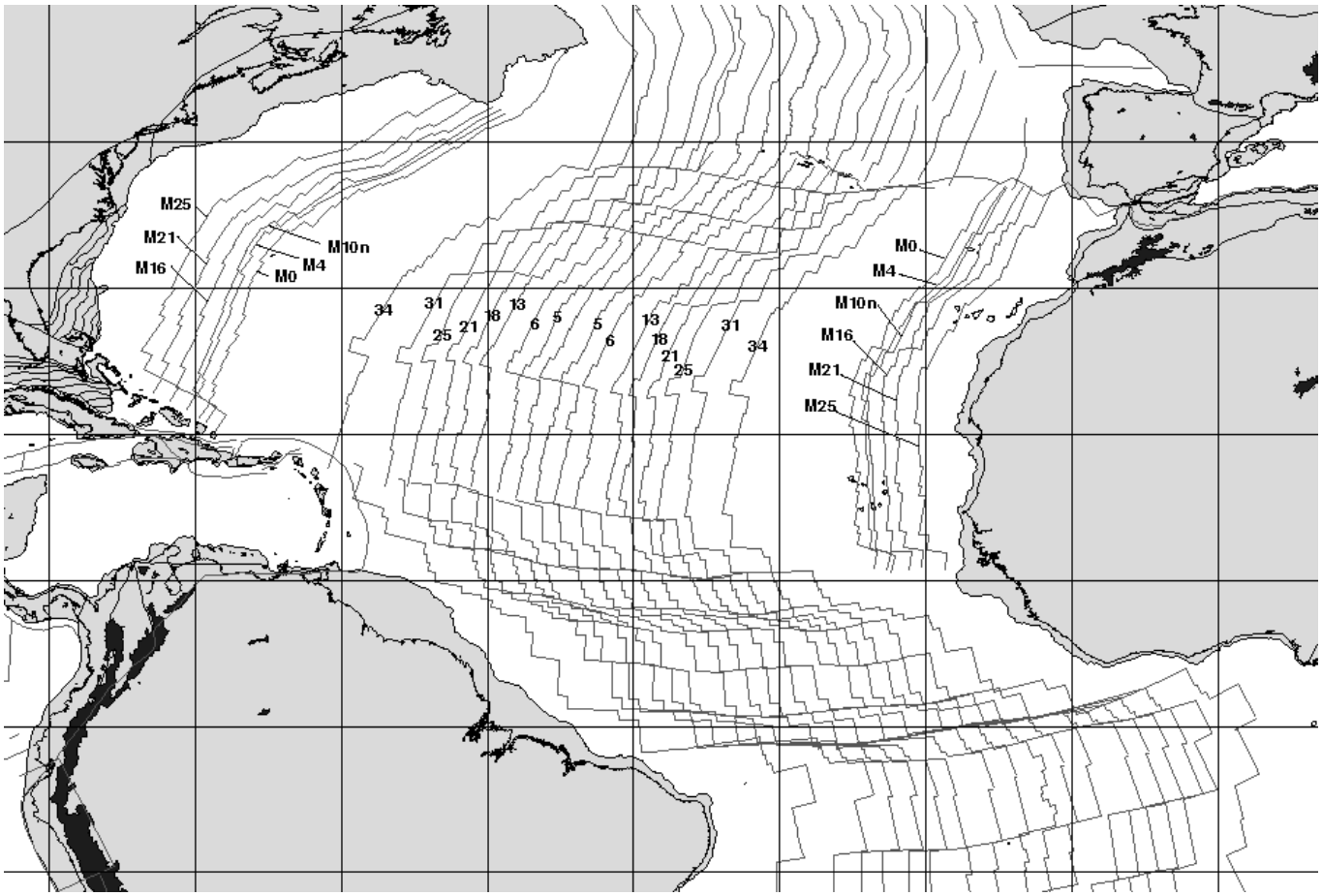

Fig. 6.5.2: Magnetic anomalies in the Atlantic ocean. The anomaly numbers indicate ages: 5 is about 10 Ma, 6 is about 20 Ma, 13 is about 33 Ma, 21 is about 47 Ma, and 34 is about 100 Ma.

Some algebra, which we omit, shows that the rotation matrix is

$$R = \begin{pmatrix} e_x^2(1-\cos\Omega_f)+\cos\Omega_f & e_x e_y(1-\cos\Omega_f)-e_z\sin\Omega_f & e_x e_z(1-\cos\Omega_f)+e_y\sin\Omega_f \\ e_x e_y(1-\cos\Omega_f)+e_z\sin\Omega_f & e_y^2(1-\cos\Omega_f)+\cos\Omega_f & e_y e_z(1-\cos\Omega_f)-e_x\sin\Omega_f \\ e_x e_z(1-\cos\Omega_f)-e_y\sin\Omega_f & e_y e_z(1-\cos\Omega_f)+e_x\sin\Omega_f & e_z^2(1-\cos\Omega_f)+\cos\Omega_f \end{pmatrix}. \quad (5)$$

The finite rotation moved two features apart that used to be at the same place. To calculate the rotation, we reverse the process mathematically and put features back together again. For example, the Atlantic Ocean opened as North and South America moved away from Eurasia and Africa. As a result, magnetic anomalies of the same age, called isochrons, on opposite sides of the Mid-Atlantic ridge are now separated (Figure 2). To describe this, we chose one plate to be fixed, and use computer programs to find a rotation that brings the isochrons on the other plate together with those on the fixed plate. Applying this rotation closes up the Atlantic part way by removing the effect of seafloor spreading during that interval. This operation going backward in time is called using a reconstruction pole and is specified by the pole's latitude and longitude and the angle of rotation. Often for convenience the term "pole" also includes the angle. Reversing this rotation gives the forward motion pole for which time goes forward and describes the opening.

Doing this for a series of isochrons gives a set of *stage poles* that describe the finite rotation over each of the time intervals. The total rotation is represented using equation 4 and multiplying at each stage by the rotation matrix for that time interval. Thus if we have two stages such that the point $\mathbf{r}$ moves first to $\mathbf{r}'$ and then to $\mathbf{r}''$,

$$\mathbf{r}' = R\mathbf{r} \quad \mathbf{r}'' = R'\mathbf{r}' = R'R\mathbf{r} = T\mathbf{r}. \quad (7)$$

where $T = R'R\mathbf{r}$ is the total rotation matrix. From the total rotation matrix, we can compute a total rotation pole and angle.

Total rotation poles have two tricky aspects. First, although they describe the total rotation between the starting and final positions, they don't specify how it took place. The actual motion occurred by a set of stages with different poles. Second, it is important to keep track of the order of the rotations. Matrix multiplication does not commute, so in general the two matrix products

$R'R$ and RR' are different. Physically this is because doing rotations in a different order gives different results. Figure 3 shows an example of a book that was rotated about the horizontal in two different orders and so ends up in different positions.

6.5.2 Comparison with infinitesimal rotations

We can think of the infinitesimal rotations that describe plate motions today as finite rotations that describe plate motions over a short time. To see that, consider how the rotation matrix (5) would look if the rotation angle Ω_f were so small that we could approximate

$$\sin\Omega_f \approx \Omega_f \quad \cos\Omega_f \approx 1 \quad 1-\cos\Omega_f \approx 0. \tag{8}$$

In this case, the matrix becomes

$$R = \begin{pmatrix} 1 & -e_z\Omega_f & e_y\Omega_f \\ e_z\Omega_f & 1 & -e_x\Omega_f \\ -e_y\Omega_f & e_x\Omega_f & 1 \end{pmatrix} \tag{9}$$

which we can write as a matrix sum

$$R = I + \varepsilon\ . \tag{10}$$

I is the identity matrix with ones on the diagonal and zeroes elsewhere, that has the property that multiplying any vector by it does not change the vector. The matrix ε contains the remaing terms involving Ω_f, so

$$I = \begin{pmatrix} 1 & 0 & 0 \\ 0 & 1 & 0 \\ 0 & 0 & 1 \end{pmatrix} \quad \varepsilon = \begin{pmatrix} 0 & -e_z\Omega_f & e_y\Omega_f \\ e_z\Omega_f & 0 & -e_x\Omega_f \\ -e_y\Omega_f & e_x\Omega_f & 0 \end{pmatrix}. \tag{11}$$

This lets us write the small change in the position of the point from $\mathbf{r}$ to $\mathbf{r}'$ in vector form as

$$\Delta\mathbf{r} = \mathbf{r}' - \mathbf{r} = (I+\varepsilon)\mathbf{r} - \mathbf{r} = \varepsilon\mathbf{r}\ . \tag{12}$$

Multiplying out the product $\varepsilon\mathbf{r}$ into its components makes this equation

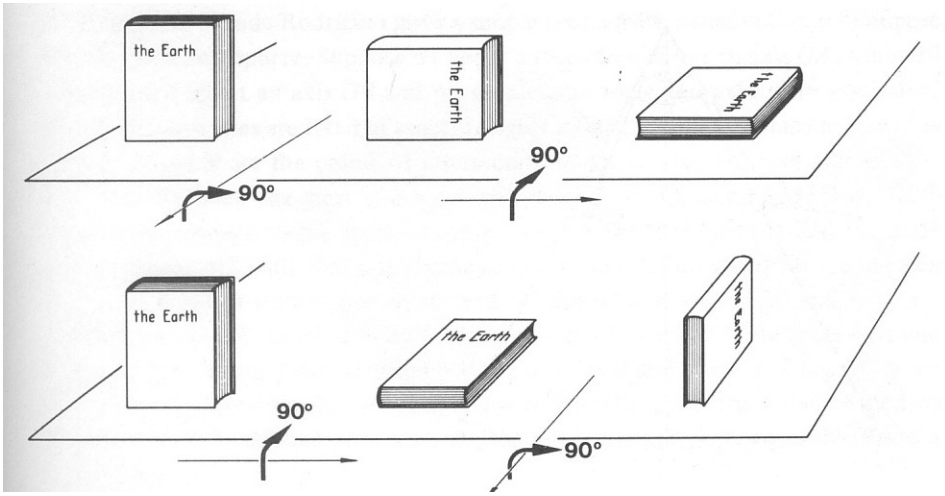

Fig. 6.5.3: Rotating a book rotated about the horizontal axes in two different orders yields two different results, illustrating that the order of rotations is important. (LePichon et al., 1973)

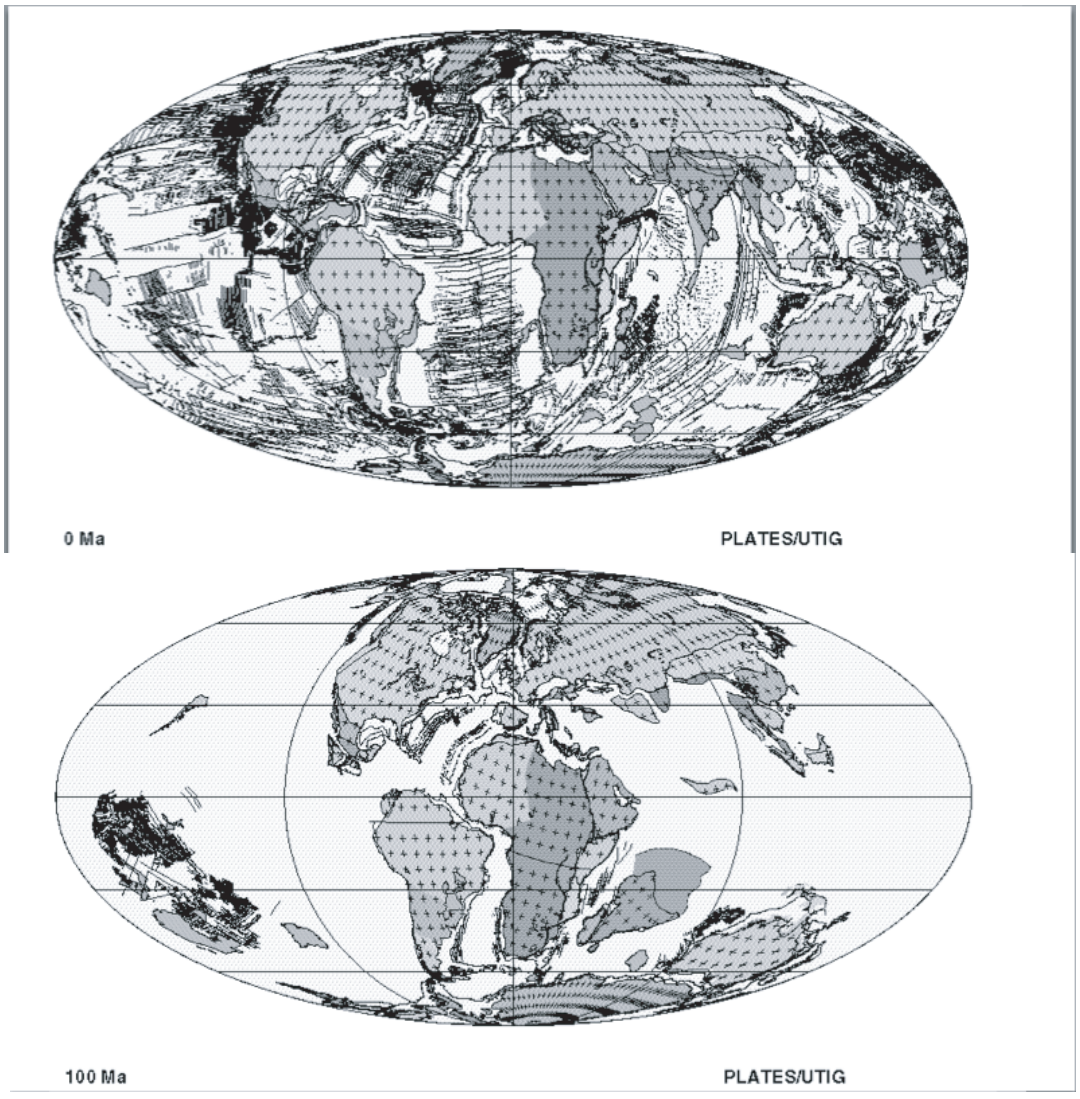

Fig. 6.5.4: Comparison of the present plate geometry to a 100 Ma reconstruction, illustrating the opening of the Atlantic. (Lawver et al., 2001)

$$\begin{pmatrix} \Delta\mathbf{r}_x \\ \Delta\mathbf{r}_y \\ \Delta\mathbf{r}_z \end{pmatrix} = \begin{pmatrix} \Omega_f(e_y r_z - e_z r_y) \\ \Omega_f(e_z r_x - e_x r_z) \\ \Omega_f(e_x r_y - e_y r_x) \end{pmatrix}. \tag{13}$$

If we divide both sides of this equation by the duration of the finite rotation, it becomes the same as the vector cross product (equation 6.3.3) equation for the linear velocity at a point **r** on a plate boundary

$$\mathbf{v} = \omega \times \mathbf{r} \ . \tag{14}$$

This is because dividing the components of the small change in position on the left side of equation 13 by the duration of the finite rotation gives the component of the linear velocity v. Similarly, dividing the finite rotation angle Ω_f by the duration of the finite rotation gives the magnitude of the angular velocity $|\omega|$, and multiplying this by the components of **e** gives the angular velocity vector ω. Thus the vector components on the right side of equation (13) are also the ones that appear in the vector cross product (equation 14). As a result, this small finite rotation is the same as the familiar infinitesimal rotation.

These ideas are illustrated by comparing rotations for the motion of Eurasia relative to North America. These are called "Euler vectors" for instantaneous motion described by infinitesimal rotations and "poles" for finite rotations. The pole location and rate in the REVEL model, derived from space geodetic data spanning seven years, is quite similar to that in NUVEL-1A, derived from data spanning the past 3 Myr. The finite rotation for the past 10 million years, 0-10 Ma, is similar because the pole location is similar and an angular change of 2.44° in 10 Myr is an average rate of 0.24°/Myr.[1] Finite rotations for the total motion over longer times differ more from the instantaneous ones. Even so, they show that over these times the opening of the Atlantic (Figure 4) has been similar to what we see today. This makes sense because the very long fracture zones extending from the active transform faults indicate that the opening of the Atlantic has occurred in a geometry similar to today's.

[1]Remember that "Ma" is millions of years before the present, whereas "Myr" is a time interval of a million years.

Table 6.5-1: Rotations for motion of Eurasia with respect to North America

	pole latitude (°N)	longitude (°E)	rate or angle
Instantaneous			
REVEL (7 yr)*	68.05	136.42	0.24°/Myr
NUVEL-1A (3 Ma)	62.41	135.83	0.21°/Myr
Finite			
(0-10 Ma)**	65.38	133.58	2.44°
(0-49 Ma)	67.19	137.74	10.91°
(0-105 Ma)	66.85	152.34	21.49°

**Sella et al.* (2002)

***Royer et al.* (1992)

Because plate motions change slowly, plate reconstructions typically form the total motion using stage poles that span about 10 million years. Even when plate motion has been fairly smooth, the stage poles give a more accurate description of the actual motion than the total pole.

In general, pole positions change over time. To see this, consider a system of three plates, i, j, and k. The Euler vector describing the motion of plate j with respect to k is just the difference of their Euler vectors with respect to plate i

$$\omega_{jk} = \omega_{ji} - \omega_{ki} \ . \tag{14}$$

This means that if the motion of j and k with respect to i stays constant over time, so will the motion of j with respect to k. Because we are dealing with relative motions, we consider plate i to be fixed and describe motions relative to it. Relative to plate i, none of the Euler vectors move. However, because plates k and j are moving relative to plate i, the Euler vector describing the motion between them must move relative to them. Thus viewed from plates j and k, the pole position for ω_{jk} is changing.